Anatomy and Interpretation of Nasal and Sinus Radiology

Joseph Gorodenker, Ameet Singh, M Reza Taheri

NASAL FOSSA, SEPTUM, AND TURBINATES

The nasal fossae are air-filled cavities separated by the vertically oriented midline nasal septum. The nasal septum is principally composed of the vomer, the perpendicular plate of the ethmoid, the quadrangular cartilage, and the membranous septum, with contribution from the palatine processes of the maxillae and the horizontal plates of the palatine bones. The columella, a strip of skin that separates the nostrils, also contributes to the anterior nasal septum.[1]

The hard palate forms the floor of the nasal cavity, of which the maxillary palatine process contributes the anterior two thirds, whereas the horizontal portions of the palatine bones form the posterior third. The bilateral cribriform plates and the fovea ethmoidalis (ethmoid roof) of the ethmoid bone form the roof of the nasal cavity. The cross-shaped ethmoid bone projects above the horizontal cribriform plate as the crista galli ("cock's comb") and extends below as the perpendicular plate of the ethmoid. The perpendicular plate articulates with the quadrangular cartilage anteroinferiorly and with the grooved vomer posteroinferiorly to form the nasal septum. The free posterior edge of the vomer divides the posterior choanae. Of note, the vomer may be bilaminar, and both it and the perpendicular plate of ethmoid may be pneumatized. The crista galli may also be aerated or may contain fat. Anterior to the crista galli lies the foramen cecum, a normally regressed developmental canal containing fibrotic tissue. Nasal dermoid cysts, nasal gliomas, and meningoencephaloceles may be associated with patency of the foramen cecum and/or a bifid crista galli. Patency may also allow venous communication from the nasal mucosa to the superior sagittal sinus, furnishing a potential route for infection.[2]
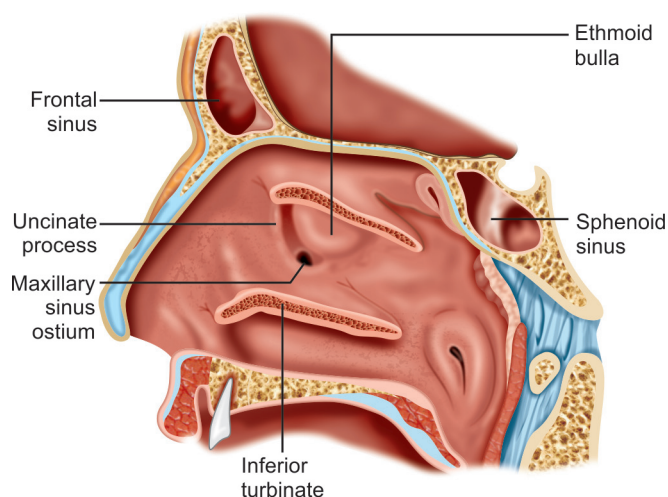

Fig. 3.1: Major landmarks of the lateral nasal wall.

The turbinates or nasal conchae (inferior, middle, superior, and the variable supreme) are paired scrolled bony projections from the lateral nasal wall, which are covered by sinus mucosa, and serve to warm and humidify inspired air (Fig. 3.1). The space below and lateral to a turbinate is the meatus named after it. The inferior turbinate has a different embryological origin (maxilloturbinal) and attaches to the medial maxillary and palatine bones. The middle turbinate and its attachments, the anterior and posterior buttresses and projecting lamellae, are important anatomic landmarks.

The anterior buttress of the middle turbinate attaches to the lateral nasal wall in the agger nasi region. The middle turbinate attaches to the ethmoid roof and cribriform plate by the vertical lamella, which extends cephalad from the anterior aspect of the middle turbinate to the lateral cribriform plate lamella (LCPL), that is, the lateral wall of the olfactory groove. The LCPL is a very thin (0.05–0.2 mm), fragile, usually vertically oriented bone
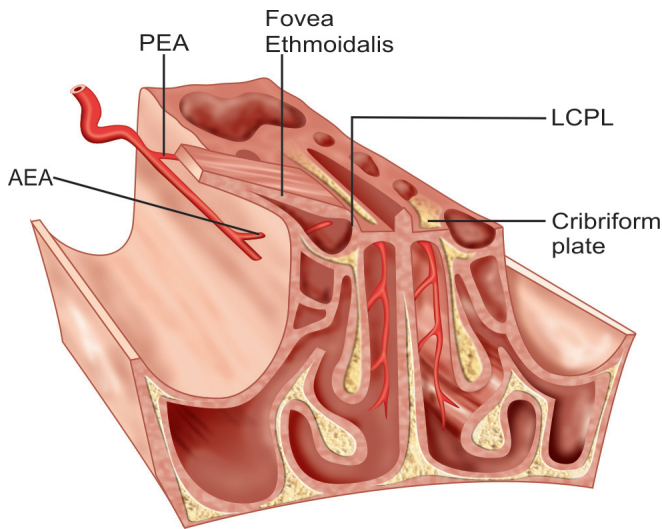
Fig. 3.2: Fovea ethmoidalis (ethmoid roof) and LCPL (lateral cribriform plate lamella). PEA: Posterior ethmoid artery; AEA: Anterior ethmoid artery.
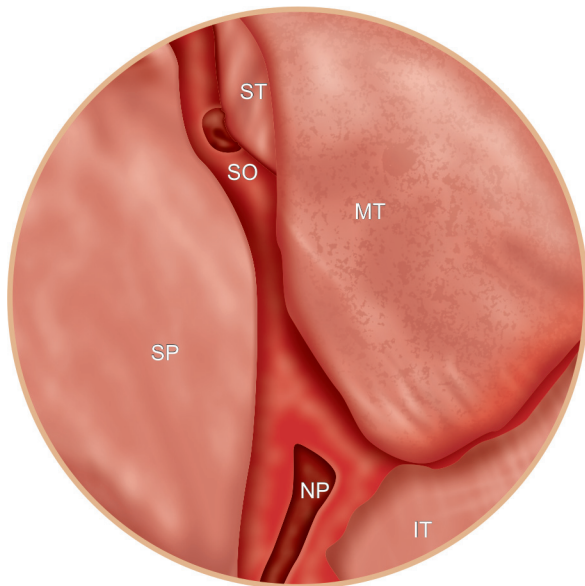

Fig. 3.3: Anterior ostiomeatal complex (OMC): uncinate process (UP), semilunar hiatus (SLH), nasofrontal recess (NFR), ethmoid bulla (EB), ethmoid infundibulum (EI), middle meatus (MM), concha bullosa (CB) = pneumatized middle turbinate, frontal sinus (FS). Also note right maxillary sinus (MS), left inferior turbinate (IT), crista galli (CG), and right lamina papyracea (LP).

The horizontal lamella (also called the basal lamella or ground lamella) marks the division between the anterior and posterior ethmoidal cells.[3] Preserving the anterior buttress, posterior buttresses and vertical lamella of the turbinate during surgery is important to prevent lateralization of the turbinate and consequent obstruction of outflow. Preservation of the inferior portion of the horizontal lamella further decreases the risk of turbinate lateralization. Pneumatization of a turbinate is called a concha bullosa (typically pneumatization of a middle turbinate by a posterior ethmoid air cell), which may cause nasal obstruction or chronic sinusitis (Fig. 3.3).

The superior and the inconstant supreme turbinate lie above and posterior to the middle turbinate, anterior to the face of the sphenoid sinus. The perpendicular attachment of the superior turbinate divides the anterior wall or face of the sphenoid sinuses into unequal medial third and lateral two thirds. The open medial third, referred to as the free intranasal surface, is bounded by the nasal septum medially, the cribriform plate superiorly, and the upper surface of the posterior choanae inferiorly. The sphenoethmoidal recess refers to the space limited by the free intranasal surface of the sphenoid and the superior turbinate (Fig. 3.4). The lateral two thirds of the anterior sphenoid sinus wall are contiguous with the posterior walls of the ipsilateral ethmoid air-cells.[4,5]

Fig. 3.4: Sphenoethmoidal recess. Superior turbinate (ST), middle turbinate (MT), inferior turbinate (IT), nasal septum (SP), sphenoid ostium (SO), and nasopharynx (NP).

that forms the medial ethmoid roof. It joins the cribriform plate medially and inferiorly, and the fovea ethmoidalis laterally and superiorly (Fig. 3.2). The horizontal lamella and posterior buttress of the middle turbinate attach to the lateral nasal wall in the sphenopalatine region.
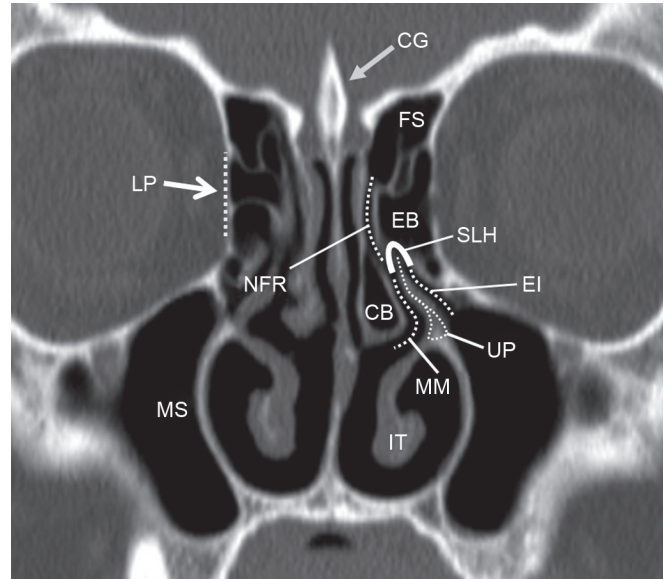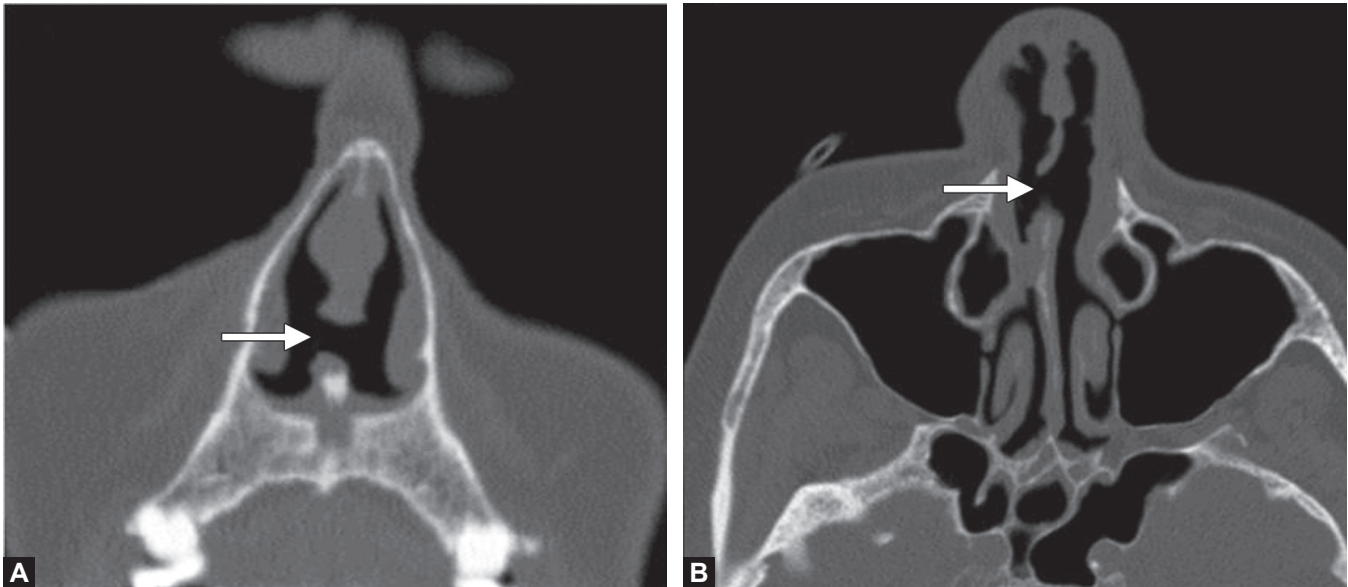
Figs. 3.5A and B: Nasal septal perforation (A) coronal and (B) axial CT images demonstrate nasal septal perforation (arrows) caused by invasive fungal disease. Absence of apparent mass suggests a non-neoplastic etiology, such as infection or granulomatous disease.

Some of the anatomic variants of the nasal fossa, which may cause sinonasal obstruction, include clinically significant nasal septum deviations, paradoxic middle turbinates, and concha bullosa of the middle or superior turbinates.

The presence of a nasal septal defect is concerning. The differential for cartilaginous nasal septal perforation is wide, ranging from trauma (including surgical resection), neoplasm (especially lymphoma, previously termed *polymorphic reticulosis* and *lethal midline granulomatosis*), typical granulomatous disease (sarcoidosis, Wegener's preferentially affect the septum), inhaled toxins (including cocaine, beryllium, chromates, etc.), and infection. Of infectious agents, TB, syphilis, and leprosy are most common, although accompanying bony sclerosis may reflect yaws. Of note, earlier in granulomatous disease, especially Wegener's but also in sarcoidosis and lymphoma, the cartilaginous septum may be swollen rather than eroded. Despite this, it is critical to recognize that any mass lesion in the nasal septal region should be presumed aggressive until proven otherwise. If a mass lesion is identified, it is important to consider its likely origin and to carefully evaluate extent. On the other hand, if no mass lesion is seen, granulomatous disease or infection should be suspected (Figs. 3.5A and B).

Diagnosis is often made by clinical history or direct visualization and histopathology; however, certain imaging features may be helpful. For example, the presence of a central diffusion-weighted imaging (DWI)-hyperintense mass on magnetic resonance imaging (MRI) is typical of T-cell lymphoma, an uncommon sinonasal tumor, whereas a hyperdense lesion on computed tomography (CT) with signal dropout on T2 weighted MRI sequences suggests fungal disease.

Nasal septal abscess is usually associated with suppressed immune status, history of trauma or postsurgical septoplasty and is rarely related to extension of dental infection or sinusitis. Early recognition of this entity is critical, as delayed management complicated by septal cartilage ischemia may lead to cosmetic deformity as well as sepsis.[6]

PARANASAL SINUS ANATOMY AND DRAINAGE

The ostiomeatal complex (OMC) is key to understanding paranasal sinus anatomy and drainage. The complex is composed of anterior and posterior ostiomeatal units.

The anterior ostiomeatal unit is composed of the frontal sinus ostium, the frontal recess, the maxillary sinus ostium, the infundibulum, and middle meatus. Together, these link the drainage systems of the frontal, anterior ethmoid, and maxillary sinuses. Mucociliary clearance in each sinus is naturally directed toward the respective sinus ostium. In the maxillary sinus, mucus from the floor of the antrum is directed toward the maxillary sinus ostium, which is typically located anteromedially. The mucus is then directed through the ethmoid infundibulum to the
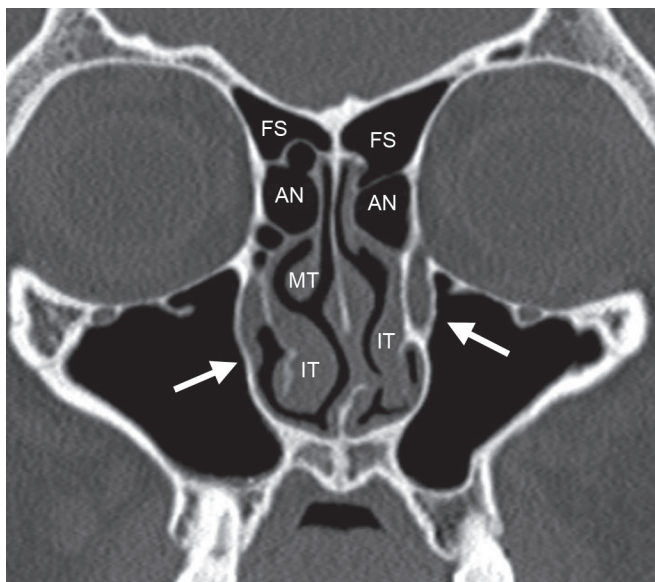
Fig. 3.6: Anterior coronal CT through the frontal sinuses (FS) demonstrates paired Agger nasi (AN) cells. Agger nasi cells are very common (90% prevalence), and represent the most anterior variable ethmoidal air cells. They are located within the lacrimal bone, and above the attachment of the middle turbinate (MT). Note arrows denoting nasolacrimal ducts draining into the inferior meati, lateral to the inferior turinates (IT).

hiatus semilunaris, and then on to the middle meatus and ultimately to the nasopharynx. The primary ostium of the frontal sinus lies medial and inferior, at the floor of the sinus. Drainage proceeds down the nasofrontal recess into the middle meatus, where it joins flow from the ipsilateral maxillary sinus. The anterior ethmoid cell ostia converge unto the middle meatus. Their drainage joins mucus from the frontal sinus (via the nasofrontal recess) and the maxillary sinus (from the maxillary ostium via ethmoidal infundibulum).[7]

Of note, some sources list the uncinate process (and/or the ethmoid bulla) as part of the anterior OMU; however, although very important to the function of the complex, this inclusion may confuse uninitiated readers as the uncinate process is a bony structure while the remainder of the listed components are air-filled spaces. Naturally, the bony walls of these listed spaces effectively contribute to the complex by outlining the air-filled cavities.

The posterior ostiomeatal unit consists of the sphenoid sinus ostium, the sphenoethmoidal recess, and the superior meatus. The posterior ethmoid air cells and the sphenoid sinus drain via the sphenoethmoidal recess into the superior meatus.

The nasolacrimal duct drains separately to the inferior meatus (Fig. 3.6). The superior, middle, and inferior meati

collectively drain to the nasopharynx. The remainder of this section reviews the relationships of these and related structures in further detail.

Frontal Sinus

The frontal sinus is contained in the frontal bone superior to the eyes in the forehead. It is formed by superior movement of anterior ethmoid cells after the age of 2 years. Growth of this sinus increases at the age of 6 years and continues until the late teenage years. The frontal sinuses are funnel-shaped structures with their ostia located in the most dependent aspect of the cavities. The posterior wall of the frontal sinus, which separates the sinus from the anterior cranial fossa, is much thinner than its anterior wall. The posterior wall lies near the superior sagittal sinus, which drains the superior cerebral and frontal *diploic veins of Breschet*. This wall represents a potential route of intracranial spread of infection with complications such as sagittal sinus thrombosis and empyema. The frontal sinus is supplied by the supraorbital and supratrochlear arteries of the ophthalmic artery. It is innervated by the supraorbital and supratrochlear nerves of the first division of the trigeminal nerve (V1).

The frontal sinuses are usually asymmetric, with the larger sinus often extending across the midline, and may contain several septations, usually better developed in larger sinuses. These septations may create partially hidden recesses, which are important to identify preoperatively, as failure to do so may result in the formation of a mucocele. Likewise, it is important to identify bullae, which are deformations of the frontal sinus floor, which may be related to contralateral frontal sinus extension or protrusion by an underlying ethmoid cell. The frontal sinuses are intimately related to adjacent anatomic structures; remodeling of the superomedial orbital margin may be related to expansile frontal sinus pathology, such as mucocele, pneumocele, or tumor.

Persistence of a metopic suture results in small or absent frontal sinuses, whereas a frontal sinus is often greatly enlarged in case of early insult to the ipsilateral frontal lobe (e.g., Dyke–Davidoff–Masson syndrome).[8] The intersinus septum, the residual frontal bone between the frontal sinuses, may be thickened or may contain focal acquired or congenital dehiscence.

Nasofrontal Recess

In broad anatomic terms, the nasofrontal recess is bordered posteriorly by the sloping anterior skull base and

anteriorly by the beak of the frontal process. Its anatomy is made complex by the wide variety of anterior ethmoidal cells that inhabit the space. Some of the more common frontal recess cells include the agger nasi cell, supraorbital ethmoid cell, interfrontal sinus septal cell, frontal bulla cell, suprabullar cell, and four types of frontal cells (types I–IV). The most prominent cells include the agger nasi cell, supraorbital cell, and the frontal cells.

Although the exact configuration and pathway of the frontal recess vary, this structure is usually bounded anteriorly by the posterior wall of the agger nasi cell (the most anterior ethmoid air cell), superiorly by the frontal sinus, medially by the LCPL (i.e., the lateral wall of the olfactory groove) and vertical lamella of the middle turbinate, laterally by the lamina papyracea, and posteriorly by the anterior wall of the ethmoidal bulla, or suprabullar recess. The risk of a cerebrospinal fluid leak from the olfactory fossa or damage to the anterior ethmoidal artery, with potential visual loss and orbital injury, make dissection in the frontal recess particularly challenging for the endoscopic sinus surgeon.

Ethmoid Sinus

The ethmoid sinuses arise in the ethmoid bone, forming several distinct air cells between the eyes. They are a collection of fluid-filled cells at birth that grow and pneumatize until the age of 12 years. The ethmoid cells are shaped like pyramids and are divided by thin septa. The basal lamella is a bony strut which extends laterally from the posterior middle turbinate to the lamina papyracea and separates the ethmoid air cells into the more numerous and smaller anterior cells and the larger and fewer posterior cells, which drain into the middle and superior meatus, respectively. Of note, the basal lamella is also attached posteroinferiorly to the crista ethmoidalis, which represents the most consistent landmark for the sphenopalatine foramen.

The ethmoid labyrinth may extend above the orbit, lateral and superior to the sphenoid, above the frontal sinus, and into the roof of the maxillary sinus.

Medially the ethmoid sinus is bound by the vertical lamella (of the middle turbinate). The lateral wall of the ethmoid sinus is formed by the lacrimal bone (anterior third), and by the lamina papyracea (posterior third), which separates the ethmoid from the orbit. The lacrimal bone, which is commonly pneumatized, lies between the ascending process of the maxilla anteriorly, where it covers the nasolacrimal duct, and the lamina papyracea and anterior ethmoid air cells posteriorly, where it covers the lacrimal process of the inferior turbinate. Superiorly, the lacrimal bone articulates with the frontal bone.

The ethmoid sinuses are supplied by the anterior and posterior ethmoidal arteries from the ophthalmic artery (internal carotid system), as well as by the sphenopalatine artery from the terminal branches of the internal maxillary artery (external carotid system).

Uncinate Process and Ethmoid Infundibulum

The uncinate process (of the ethmoid) is a cutlass-shaped superior bony projection. The uncinate lies lateral to the middle turbinate, articulates with the inferior turbinate, and attaches to the posterior wall of the lacrimal bone anteriorly. This is useful in locating the nasolacrimal duct, which drains into the anterior superior aspect of the inferior meatus (Fig. 3.6).

The uncinate process is a critical bony structure of the lateral nasal cavity. With the ethmoid bulla it contributes to the ethmoid infundibulum and the hiatus semilunaris, a common drainage pathway for the anterior ethmoid and maxillary sinuses (and potentially the frontal sinus; see below). Hence, its anatomic configuration may cause anterior ethmoid, frontal recess, and/or infundibular (maxillary) sinus obstruction. A pneumatized uncinate, typically related to extension of an agger nasi cell, is termed an uncinate bulla. This may cause obstruction but is relatively uncommon.

The unfortunately named ethmoid infundibulum is a channel that drains the maxillary sinus. It lies between the uncinate process (caudally and medially) and the inferomedial margin of the orbit (cranial and lateral). The infundibulum drains to the hiatus semilunaris, a space that lies medial and superior to the infundibulum, and above the uncinate process (see below). If the free edge of the uncinate process deviates laterally, it may narrow or obstruct the hiatus semilunaris and/or the infundibulum. The infundibulum may also be narrowed or obstructed by Haller cells (see below).

The uncinate process usually attaches to the medial orbital wall superiorly but may attach to the skull base or the middle turbinate, and these various patterns of attachment are variously categorized[7] (e.g., Landsberg and Friedman); however, essentially the site of superior attachment of the uncinate influences the drainage pattern of the frontal sinus in relation to the ethmoidal infundibulum (Figs. 3.7A to C):

- If the uncinate process bends laterally (most frequent configuration) and inserts superiorly into the lateral nasal wall (a common location of agger nasi cells) or the lamina papyracea, the ethmoidal infundibulum is separated from the frontal recess. In this case, the
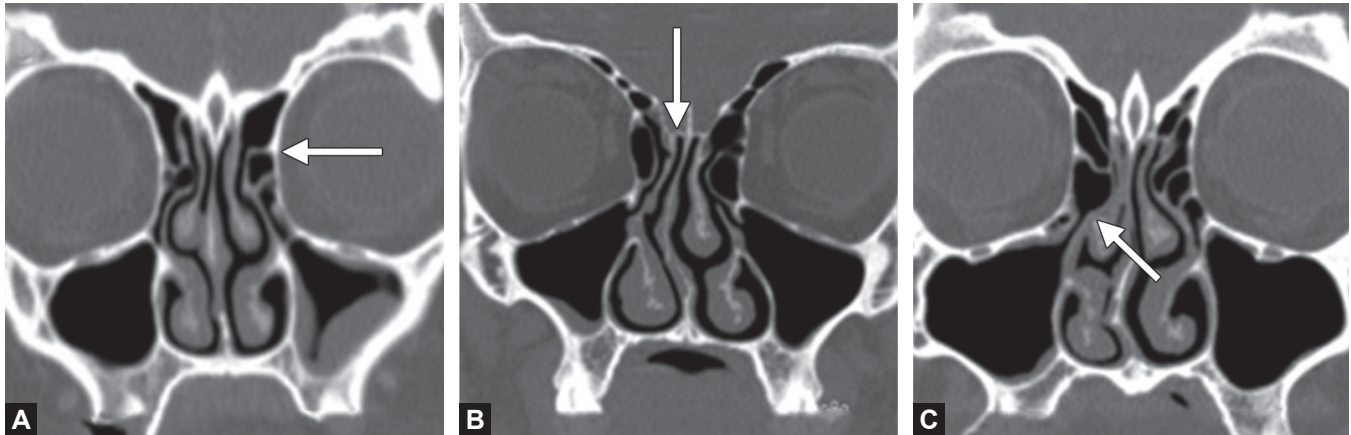
Figs. 3.7A to C: The superior attachment of the uncinate process (white arrows) affects the drainage pattern of the frontal sinus. (A) Attachment to the lamina; (B) Attachment to cribriform plate/skull base; (C) Attachment to middle turbinate.

frontal recess drains separately into the middle meatus, medial to ethmoidal infundibulum. The resultant blind-ending superior portion of the ethmoidal infundibulum is termed the recessus terminalis.

- If the uncinate process extends to the ethmoid roof, the frontal sinus drains directly into the ethmoid infundibulum. Excessive traction during uncinectomy in such configuration may cause injury to the ethmoid roof and result in cerebrospinal fluid (CSF) leak or other complications. If the uncinate process extends to the roof of the anterior ethmoid, the superior infundibulum is closed superiorly, and the infundibulum drains via the posterior middle meatus.
- If the uncinate process turns medially and attaches to the middle turbinate, the frontal sinus drains into the ethmoid infundibulum.

Ethmoid Bone

The medial portion of the ethmoid bone is a cruciate membranous bone that is composed of the crista galli, the cribriform plate and the superior portion of the nasal septum. The crista galli is a thick portion of bone, shaped like a cock's comb, that projects superiorly into the cranial cavity and serves as an attachment of the falx cerebri. If pneumatized, the crista galli air cell drains into either the left or right frontal sinus. The cribriform plate contains several perforations that transmit olfactory fibers to the middle turbinate, superior turbinate, and the superior nasal septum. The perpendicular plate of the ethmoid articulates with the quadrangular cartilage anteroinferiorly and with the vomer posteroinferiorly to form the nasal septum.

Ethmoid Roof

The vertical lamella (of the middle turbinate) divides the anterior skull base into the cribriform plate medially and the roof of the ethmoid, or fovea ethmoidalis, laterally.

The fovea ethmoidalis slopes inferiorly when traveling in an anterior-to-posterior or lateral-to-medial direction along the skull base. Understanding this orientation is important for preventing inadvertent entry into the skull base during endoscopic sinonasal procedures. The roof of the ethmoid is primarily composed of a thicker horizontal portion, called the orbital plate of the frontal bone, and a thinner vertical portion, called the LCPL (also known as the lateral wall of the olfactory groove). The height of the LCPL defines the depth of the olfactory cleft where dura is closely adherent to the bone. The bony thickness of the LCPL ranges from 0.05 to 0.2 mm and provides little resistance to injury (*see* Fig. 3.2).[3]

The depth of the olfactory cleft may be graded by the Keros system as Type I (1–3 mm), Type II (3–7 mm), or Type III (8–16 mm). Deeper olfactory clefts are at greater risk during surgery, including CSF leak, pneumocephalus, or intracranial injury.[9] The most common location of iatrogenic CSF leak is the thinnest portion of the LCPL in the region of the anterior ethmoid artery (AEA), which courses along the anterior ethmoid roof, from the orbit to the olfactory groove.

Of note, an anatomic variant exists in which the orbital plate is relatively thin and the LCPL runs in a more horizontal direction. A great risk of inadvertent injury exists if the surgeon perceives the thinner orbital plate to be part of a superior ethmoid cell, rather than the skull base.

Ethmoid Bulla and Semilunar Hiatus

The ethmoid bulla is the largest of the anterior ethmoidal cells and is a constant landmark during endoscopic surgery. It lies posteromedial to the uncinate process, superior to the ethmoidal infundibulum, and anterior to the basal lamella (of the middle turbinate), which separates the anterior from the posterior ethmoidal cells.

The ethmoid bulla often extends cephalad all the way to the skull base, however, it may be separated from the skull base by a suprabullar cell or a cleft named the suprabullar recess. Alternatively, it is sometimes attached to the skull base via the bulla lamella. The anterior ethmoidal artery usually courses superomedially in the region of the bulla lamella.

The air space between the inferolateral surface of the ethmoidal bulla and the superior surface of the uncinate process is called the hiatus semilunaris (or semilunar hiatus). This common space joins the infundibulum (and potentially the nasofrontal recess, depending on the config-uration of the uncinate process) with the middle meatus, allowing maxillary sinus (and possibly frontal sinus) mucus to drain with the anterior ethmoid cells into the middle meatus, and then to the nasopharynx (*see* Fig. 3.3).

If the ethmoidal bulla has a posterior surface separate from the basal lamella, the space between them is called the retrobullar recess or sinus lateralis. The retrobullar recess may communicate with the suprabullar recess, a space that may exist between the superior surface of the ethmoidal bulla and the fovea ethmoidalis (skull base).

Haller Cell (Infraorbital Ethmoid Cell)

The Haller cell, or infraorbital ethmoid cell, is an anterior ethmoidal cell that pneumatizes into the maxillary sinus ostium just below the medial floor of the orbit (Fig. 3.8). A Haller cell may contribute to recalcitrant maxillary sinus disease in some cases of chronic sinusitis. This is usually secondary to mucosal inflammation of the common wall between the Haller cell and the maxillary sinus ostium.

Patterns of Sinus Disease

Sinus disease often takes the form of a recognizable pattern that reflects the location of obstruction. Obstruction at the middle meatus results in the OMC pattern (per Sonkens' classification[10]) and involves the maxillary sinus, the anterior ethmoid group and variably the frontal sinus, depending on the insertion of the anterior uncinate
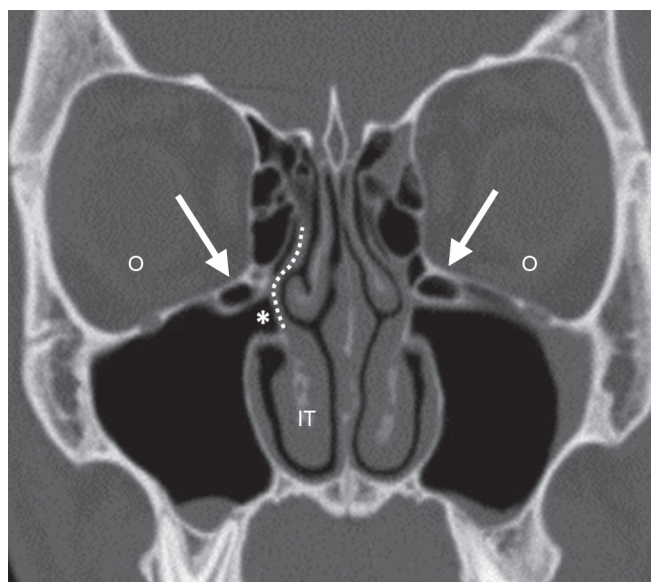

Fig. 3.8: Haller cells (arrows) are anterior ethmoid air cells which pneumatize and potentially narrow the maxillary sinus ostium (*) just below the medial floor of the orbit (O). Note the relationship of the Haller cell on the right to the uncinate process (dashed line).

process, as discussed above. Obstruction at the middle meatus may be related to mucosal edema, structural lesions such as concha bullosa or septal deviation, or mass effect from a benign or malignant process.

The frontal recess inflammatory pattern, a variant of the OMC pattern above, refers to the isolated involvement of the frontal sinus in case of isolated involvement of a frontal recess or direct drainage of the frontal recess into the middle meatus.

The infundibular pattern of sinus disease refers to the isolated obstruction of the ethmoid infundibulum and/or the maxillary sinus. In this pattern, the frontal and/or ethmoid sinuses are not involved. The underlying etiology may likewise include mucosal edema, polypoid lesions or structural lesions such as Haller cells.

Not uncommonly, diffuse obstruction develops, spar-ing the inferior meatus, with extensive polyps throughout the nasal cavity and the paranasal sinuses (Figs. 3.9A and B). This sinonasal polyposis pattern should be dis-tinguished from the sporadic pattern, which refers to no apparent pattern of paranasal sinus pathology.

Agger Nasi Cell

The agger nasi cell, when present, is the most anterior of the ethmoidal cells (*see* Fig. 3.6). Located within the lacrimal bone, it is found in over 90% of CT scans. Agger nasi cells are found medial to the nasolacrimal duct,
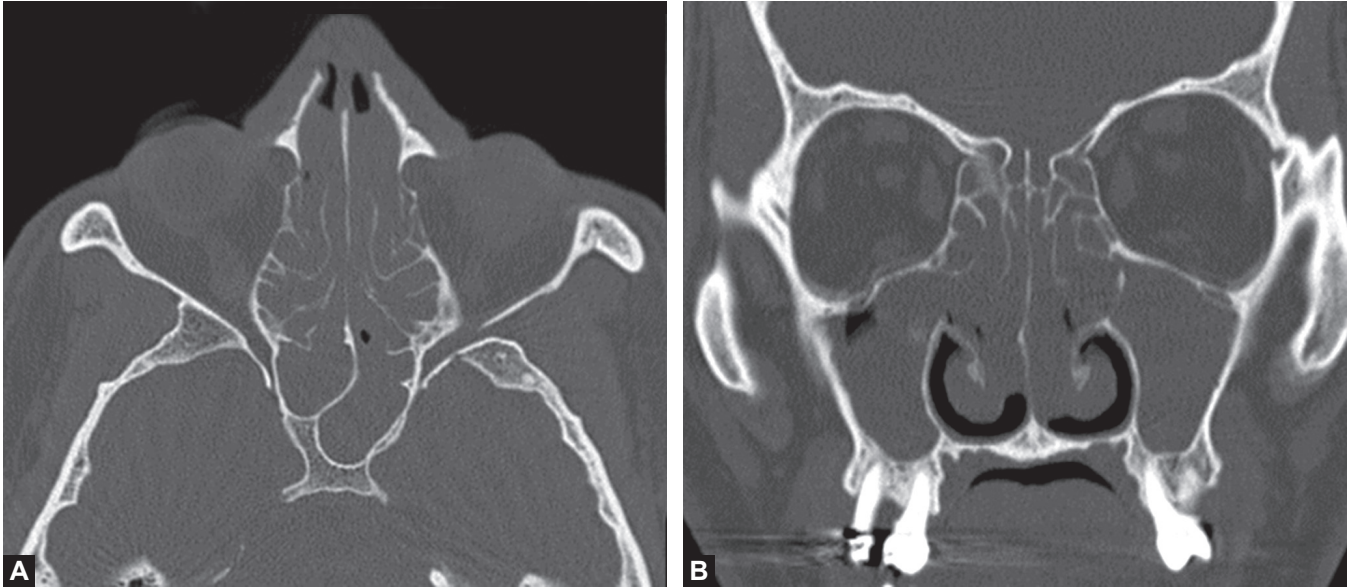
Figs. 3.9A and B: Diffuse polyposis. (A) Axial and (B) coronal CT demonstrate generalized homogeneous opacification of the sinuses with no evidence of bony involvement (no erosion, bulging, or dehiscence). The appearance of convex, outward margins to the fluid density in the opacified structures suggests polyposis rather than mere sinusitis.

and anterior and superior to the anterior buttress of the middle turbinate. The medial wall and roof of the agger nasi cell often lie in close association with the vertical lamella of the middle turbinate and the anterior skull base, respectively, whereas the posterior wall often represents the anterior face of the nasofrontal recess. The superior surface (or cap) of the agger nasi cell, if left in place during frontal recess surgery, may contribute to iatrogenic frontal sinus obstruction.

Frontal Sinus Cells

Four types of frontal sinus cells may pneumatize above the agger nasi cell, and potentially contribute to the complexity of frontal recess anatomy. A type I frontal sinus cell lies above the agger nasi cell. A type II frontal sinus cell is a configuration of two cells stacked above the agger nasi cell. A type III cell is a large frontal sinus cell that pneumatizes into the frontal sinus and occupies nearly 50% of the sinus. Finally, a type IV frontal sinus cell is a single isolated cell that exists completely within the frontal sinus and has no connection to the frontal recess.[7]

Supraorbital Ethmoid Cell

The supraorbital ethmoid cell is an anterior ethmoidal cell that pneumatizes into the orbital plate of the frontal bone, occasionally involving the lateral wall of the orbit. When extensively pneumatized, this cell may be mistaken for the frontal sinus or a septate frontal sinus.

Maxillary Sinus

The maxillary sinus is the largest of the paranasal sinuses. It is situated within the body of the maxillary bone below the orbits. The shape of the sinus is a pyramid with the base along the nasal wall and the apex pointing laterally toward the zygoma. Embryologically, it is the first sinus to form and usually grows symmetrically. Its growth is biphasic, where the first phase occurs during the first 3 years and the second during years 6–12. Pneumatization is initially directed horizontally and posteriorly during the first phase and inferiorly toward the maxillary teeth during the second phase.

Maxillary hypoplasia is uncommon, and may be related to prior trauma, infection, surgical intervention, irradiation, or underdevelopment related to branchial arch anomalies (e.g., Treacher-Collins s., mandibulofacial dysostosis) or erythropoetic demand, such as thalassemia major.[8]

The medial wall of the maxillary sinus is the inferolateral wall of the nasal cavity, whereas the posterolateral wall separates the sinus from the pterygopalatine fossa and infratemporal fossa. The roof of the maxillary sinus is also the floor of the orbit.

The natural maxillary sinus ostium varies in precise location, but usually lies at the superior aspect of the medial wall, and measures up to 4 mm in diameter. It drains indirectly into the nasal cavity via the infundibulum

(see *Ostiomeatal Complex* above). Multiple structures contribute to the maxillary hiatus (ostium): portions of the ethmoid bone (forming the uncinate process), the perpendicular plate of the palatine bone (posteriorly), the lacrimal bone (anterior and superior), and inferior turbinate (inferior).

The lateral nasal wall has two areas deficient in bone that lie anterior and posterior to the uncinate process. These areas are called fontanelles, or accessory ostia that may be confused with the natural maxillary sinus ostium. Although sometimes functional, these ostia rarely function as the true ostium because the mucociliary clearance pattern of the maxillary sinus preferentially flows to the natural ostium. A posterior ethmoid cell can invade the posterior maxilla and divide the maxillary antrum into anterior and posterior compartments, which may drain separately into the nasal fossa via accessory ostia. Rarely, the antrum is divided by a horizontal or vertical septum.

The maxillary nerve (canal) lies within the maxillary sinus roof, diving anteriorly to exit 1 cm below the inferior orbital rim on the anterior face of the maxilla via the infraorbital foramen. The thinnest portion of the anterior maxillary wall is above the canine tooth, called the canine fossa. This area is an ideal entry site for addressing various disease processes of the maxillary sinus if endoscopic surgery is not sufficient. The maxillary sinus is supplied by branches of the internal maxillary artery, which include the infraorbital, alveolar, greater palatine and sphenopalatine arteries. It is innervated by branches of the mandibular nerve (second branch of the trigeminal), the infraorbital nerve and the greater palatine nerves.

The maxillary sinuses contain several named recesses. The lateral or zygomatic recess extends into the malar eminence of the zygoma. The tuberosity recess extends inferiorly and posterior to the third maxillary molar. The alveolar recess extends to the alveolar process of the maxilla. The variable palatine recess extends into the hard palate. Notably, the inferior pneumatization of the sinus is intimately related to tooth eruption; bone overlying the tooth roots may be dehiscent with only mucosal covering.

Sphenoid Sinus

The sphenoid sinuses are a large pair of paranasal sinuses located in the sphenoid bone posterior to the ethmoid sinuses. These paired sinuses develop separately from the nasal capsule of the embryonic nose, often divided by a single vertical intersinus septation. However, multiple complete and incomplete bony septations, with vertical, horizontal, or oblique orientations, may further subdivide the sinus. In one radiologic study, 80% of sphenoid sinuses were found to have a single sphenoid septation, and 20% were found to have a double septation. These septations often localize to the carotid artery, underscoring the importance of atraumatic dissection to avoid a catastrophic vascular injury.

Sphenoid Pneumatization Patterns

Pneumatization of the sphenoid sinus is highly variable and can extend as far as the clivus inferiorly, the sphenoid wings laterally and the foramen magnum inferiorly. Pneumatization of the sphenoid sinuses is rarely absent, with lack of pneumatization suggesting underlying abnormal erythropoetic demand (e.g., thalassemia).[9] Pneumatization of the vast majority of sinuses reaches the sella turcica by the age of 7 years. The major pneumatization patterns for sphenoid sinus include sellar (55%), presellar (20%), conchal (3%), and postsellar (22%) (Fig. 3.10).[11]

A sellar sphenoid sinus has pneumatization anterior and inferior to the sellar prominence. A presellar sphenoid sinus has pneumatization only anterior to the sella. A conchal sphenoid sinus has minimal to no pneumatization, and poses the greatest anatomic challenge to the endoscopic management of sphenoid, pituitary, or anterior skull base pathology. A postsellar configuration consists of presellar pneumatization followed by a smaller pneumatization behind the sella. This pattern is important to recognize during endoscopic skull base surgery.

The degree of sphenoid sinus pneumatization determines the relative location of the foramen rotundum and vidian canal, which may lie outside the sinus or protrude into the lower lateral sinus wall. Likewise, the cartotid artery may lie outside the sinus, lie within a sinus septum or may be covered by a partially dehisced wall, predisposing it to injury. It is thus critical to identify the carotid artery on preoperative imaging.[12] The sphenoid sinus commonly (50%) extends laterally to involve the greater sphenoid wing (lateral recess), underlying the middle cranial fossa and the posterior orbital wall. The pterygoid process is less commonly pneumatized (25%). These represent common sites of spontaneous CSF leak into the sphenoid sinus.[13]

Onodi Cell

The Onodi, or sphenoethmoid cell, is a posterior ethmoidal cell that pneumatizes the sphenoid bone, posterior, lateral, and superior to the sphenoid face. It is present
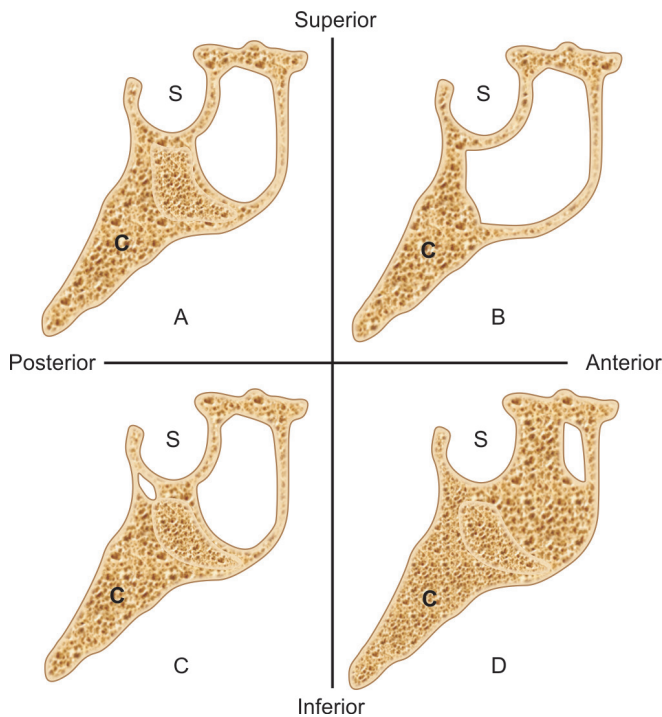
Fig. 3.10: Sphenoid pneumatization patterns: (A) sellar, (B) presellar, (C) conchal, and (D) postsellar. Note the clivus (C) and sella (S).

in 7–25%, with higher prevalence in patients from the Far East and the Indian subcontinent. Recognizing the presence of this cell before and during endoscopic sinus or skull base surgery is important. An Onodi cell may encompass the optic nerve laterally in the posterior ethmoid sinus, making it potentially vulnerable to injury. The presence of an Onodi cell places the sphenoid sinus in a more medial and inferior position, thereby increasing the risk of intracranial penetration if the surgeon expects the sinus to be behind the last posterior ethmoid cell.

Endoscopic Sphenoid Sinus Anatomy

The endoscopic anatomy of the sphenoid sinus has several anatomic landmarks that are important for the endonasal endoscopic surgeon. The midline posterior wall of the sphenoid sinus reveals the sellar protuberance, inferior to which lies the clivus, separated by the sellar–clival junction. Superior and anterior to the sella lies the planum sphenoidale, separated by a thick ridge of bone called the tuberculum sellae, which corresponds to the chiasmatic sulcus intracranially.

The lateral wall of the sphenoid sinus reveals four prominences and three depressions. The prominences,

from superior to inferior, are the (1) optic nerve, the (2) parasellar internal carotid artery, the (3) maxillary division, V2 and the (4) mandibular division, V3 of the trigeminal nerve. The three bony depressions of the lateral sphenoid sinus wall are the lateral opticocarotid recess, the depression between the cavernous sinus apex and the maxillary nerve, and the depression between the maxillary and mandibular divisions of the trigeminal nerve (Fig. 3.11).

In addition, the space medial to the junction between the optic nerve and the carotid arteries, called the medial opticocarotid recess, has been labeled the "anatomic keyhole" in endonasal skull base surgery.[14] Nearly 25% of patients may have a bony dehiscence over critical structures such as the optic nerve and the carotid artery. Caution must be exercised in the removal of these septations in order to prevent visual or vascular injury.

Sphenoid Ostium and Sphenoethmoid Recess

The natural sphenoid sinus ostium is located 1.5 cm superior to the posterior choanae on the anterior sphenoid sinus wall. The natural ostium is elliptical in shape and is found in close association with the superior turbinate in the sphenoethmoid recess. In 83% of cases, the ostium is located medial to the superior turbinate and may be visualized with gentle lateralization of the superior turbinate. To further aid craniocaudal localization, if the superior turbinate is divided into horizontal thirds, the natural ostium lies at the junction of the inferior and middle thirds of the superior turbinate.

The sphenoethmoid recess is the narrow vertical corridor enclosed by the septum medially and the superior turbinate laterally. It is defined superiorly by the cribriform plate and inferiorly by the floor of the nasal cavity. The natural sphenoid ostium drains into this corridor, as do the posterior ethmoid cells. Thereafter, mucus continues to the superior meatus, and on to the nasopharynx.

RADIOLOGIC APPROACH

Computer-aided tomography is a volumetric modality that is based on the differential attenuation of X-rays by tissues. Although plain film offers higher spatial resolution, CT benefits from its superb and 3D-capable anatomic definition and density discrimination. CT is additionally valuable as a screening modality for its sensitivity to early osseous involvement, a critical feature in the characterization of sinusitis and sinonasal lesions.[15]
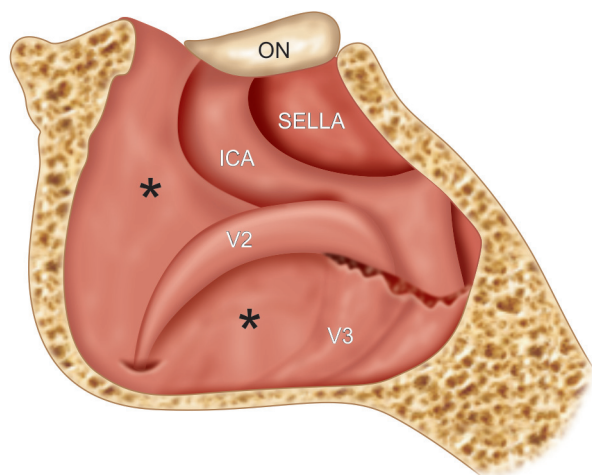
Fig. 3.11: Bony depressions* of the lateral sphenoid sinus wall. Optic nerve (ON), internal carotid artery (ICA), V2 = maxillary nerve, V3 = mandibular nerve.

CT Bone

Effective evaluation of abnormal bone relies on acquiring images with an appropriate bone kernel, a scanner-specific bone-optimized algorithm, and using suitable viewing windows. Bones on a sequence acquired with a "soft-tissue" kernel will appear diffusely sclerotic and thickened, and fine osseous changes may not be apparent. Likewise, fine osseous changes are also difficult to appreciate on contrast-enhanced CT images, which are usually acquired with a soft-tissue kernel.

Bone Thickening and Sclerosis

Bone thickening, as related to the paranasal sinuses, generally reflects a benign process, most frequently chronic sinus disease, whether allergic, odontogenic or polypoid, and may be focal or diffuse. Sclerosis typically accompanies bone thickening, and is recognized by the hyperintensity, or brightness, of dense bone on CT. The presence of sclerosis also suggests an indolent, benign process, whether a reaction to chronic inflammation or a pathologic imbalance between osteoblastic and osteoclastic activity. The recognition of bone thickening and sclerosis often benefits from asymmetry.

Chronic sinus obstruction commonly results in both periosteal thickening and sclerosis of the involved sinus walls. This may affect a single sinus due to ostial obstruction or may present in a pattern involving several sinuses (see *Patterns of Sinus Disease*). Occasionally, a mass may cause obstruction of only a portion of a sinus with focal underlying mural thickening and sclerosis. Such

an obstructing mass would most likely be benign, given the necessarily indolent, chronic nature of the associated findings, and may represent a polyp or a fungus ball. Aside from a suggestive rounded contour or subtly higher internal density such a lesion may be difficult to distinguish from adjacent trapped mucus secretions on non-contrast CT imaging.

Occasionally, chronic obstruction results in a pattern of "silent sinus," an incompletely understood sclerotic collapse or atelectasis of the maxillary sinus, associated with cosmetic deformity and enopthalmos (Fig. 3.12).[16] In contrast, the apparent absence of a sinus likely reflects a congenital abnormality, and may be associated with other significant clinical findings (e.g. thalassemia, Kartagener syndrome, Trisomy 21).

Benign Bony Expansion

Reactive bony thickening should be distinguished from bony expansion, a characteristic appearance of several uncommon but benign entities. Fibrous dysplasia is a rare process that represents abnormal fibrous bone tissue filling and expanding the medullary cavity of bone (Figs. 3.13A and B). When present, fibrous dysplasia commonly affects bones of the skull and has a typical hazy "ground-glass" appearance on CT. It is usually limited to one bone (80%), although polyostotic forms occur and may be associated with McCune-Albright syndrome.

Paget's disease (of the bone, i.e. *osteodystrophia deformans*) may also simulate thickening or sclerosis related to sinusitis. This is a benign multistage process of imbalanced bone formation and resorption, resulting in expanded characteristically heterogeneous "woven-bone" appearance, although imaging findings vary with disease stage.

Other lesions that have more focal appearance of bony expansion include osteoma, one of the most common benign tumors of the nose and paranasal sinuses. An osteoma represents a densely sclerotic protruding bone growth which may cause obstruction or deformity (commonly proptosis) if large or unfortunately located.

Odontogenic fibromyxomas are exceedingly rare benign tumors, usually affecting the posterior mandible but occasionally the maxilla, from where they may extend cephalad into the maxillary sinus. They do not have a characteristic appearance on CT and have been described as having a "lacelike," "honeycomb," and "soap bubble" appearance, but also simply "lucent," a generic term for low density on CT.[17] Hemangiomas are much more common, and may have a similar appearance.

Thinning and Remodeling

Thinning and remodeling of the osseous sinonasal structures, whether diffuse or focal, is associated with benign processes, such as mucoceles, allergic fungal sinusitis
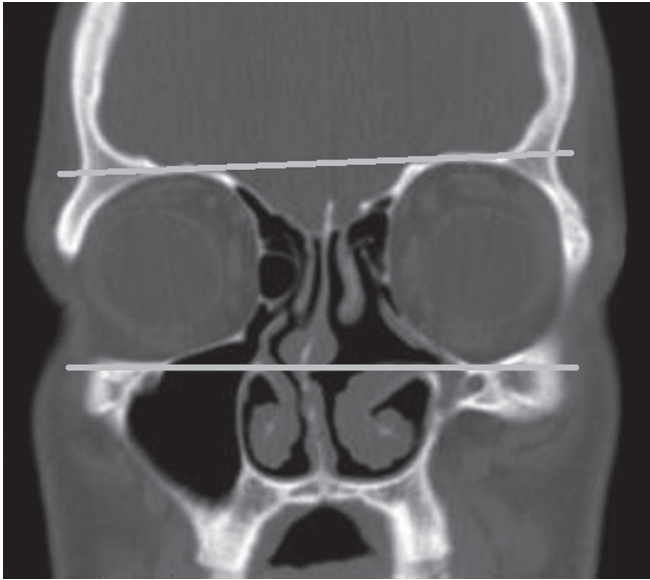

Fig. 3.12: "Silent Sinus" syndrome. Coronal CT demonstrates a shrunken left maxillary sinus with increased craniocaudal diameter of the left orbit as compared with the right (note guide-lines diverging to the left). These are the findings of "silent sinus," maxillary sinus atelectasis that is often accompanied by deformity of the orbital floor, or enopthalmos. This should be distinguished from maxillary sinus hypoplasia, which has normal-appearing orbits.

(AFS) and polyposis.[17] The diffuse expansion of a fluid-filled air cell is a common appearance of a mucocele, which represents a mucus-filled sac that slowly fills up with mucus. Mucoceles should be distinguished from the much more common mucus retention cysts, fluid-filled sacs that do not typically cause mass effect and usually do not remodel adjacent bone. Most mucus retention cysts remain unchanged or shrink over time but rarely may become displaced and cause obstruction. Focal remodeling may also reflect a benign polyp (Figs. 3.14A and B). An "antrochoanal" polyp, referring to its maxillary sinus origin, often causes isolated medial bulging of the medial maxillary sinus wall.

Notably, certain osseous structures are less able to remodel in response to chronic pressure. These include the floor of the anterior cranial fossa and the skull base. In these locations, mucoceles and AFS instead cause pressure demineralization, which appears as lucent or absent bone (Figs. 3.15A and B).[18] Pressure demineralization is expected to have smooth, mildly bulging margins and may result in appearance of dehiscence or "a hole," which may reverse on removal of the offending process. Pressure demineralization must be carefully distinguished from erosion, which suggests an aggressive or malignant process.

Erosion

Osseous erosion is pathognomonic for an aggressive process, which may reflect neoplasm or infection, and
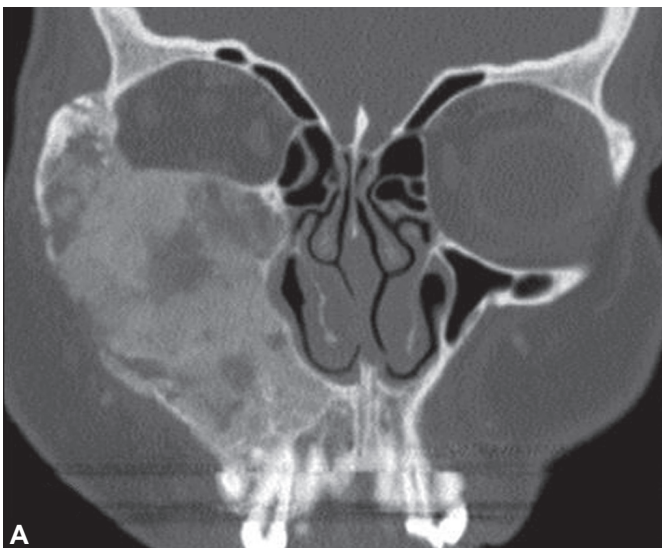
Figs. 3.13A and B: Fibrous dysplasia. (A) Coronal and (B) axial CT demonstrate heterogeneous sclerotic bone expansion of right maxillary marrow space, extending beyond the sinus, with characteristic "ground-glass" appearance that is pathognomonic for fibrous dysplasia, a benign process.
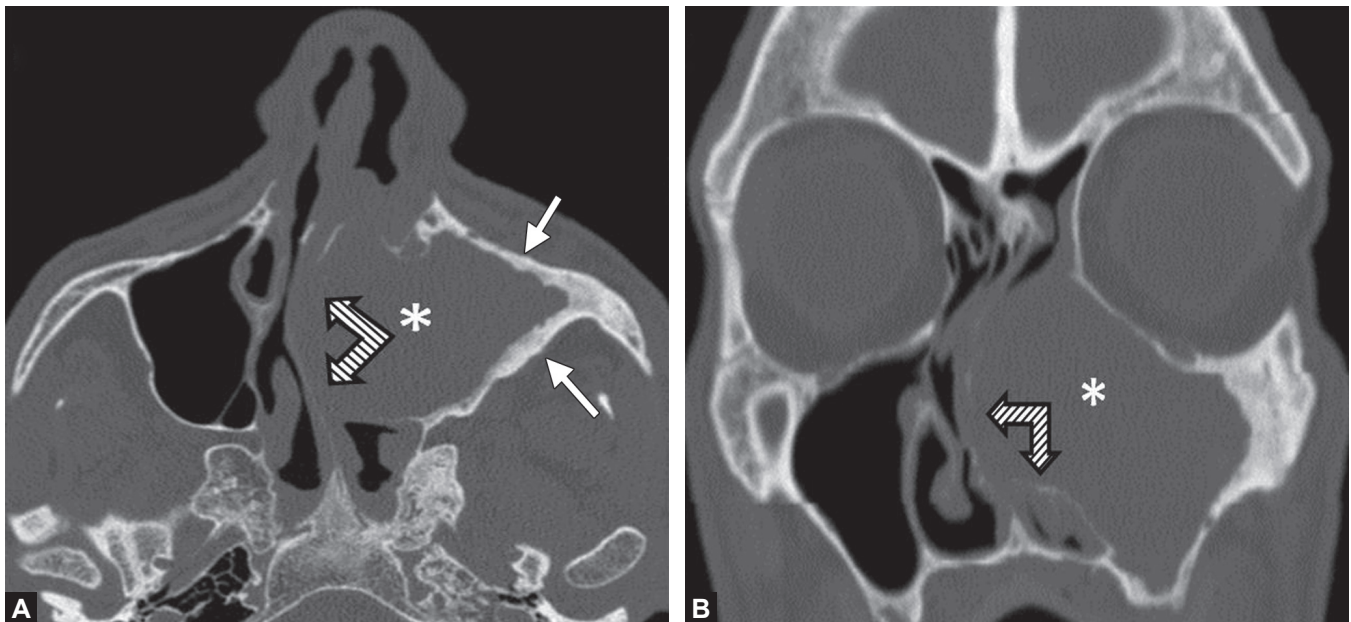
Figs. 3.14A and B: (A) Axial and (B) coronal CT demonstrate periosteal thickening (white arrows), implying a chronic obstructive process. There is focal remodeling (double arrows) of the nasal septum, the medial wall of the left maxillary sinus, and the left middle and inferior turbinates. This represents indolent mass effect, related to chronic obstruction by an antrochoanal polyp (*).

Figs. 3.15A and B: Pressure demineralization. (A) Axial CT demonstrates marked expansion of the right sphenoid sinus (black arrows), a finding fairly specific for mucocele. High density on CT (*) suggests fungal colonization, further supported by (B) T2 signal loss or "drop-out." Postoperative CT better demonstrates the smooth demineralization consistent with a non-aggressive process (not shown).

is best identified as absent bone with sharp or shaggy, irregular margins (Fig. 3.16). Fine irregular calcifications may be seen in place of eroded bone, which may represent residual fragments or tumoral calcification.

Erosion must be carefully distinguished from pressure demineralization or remodeling, which are characterized by smooth contours and bulging, implying chronicity and hence benignity. Appearance of bone destruction without
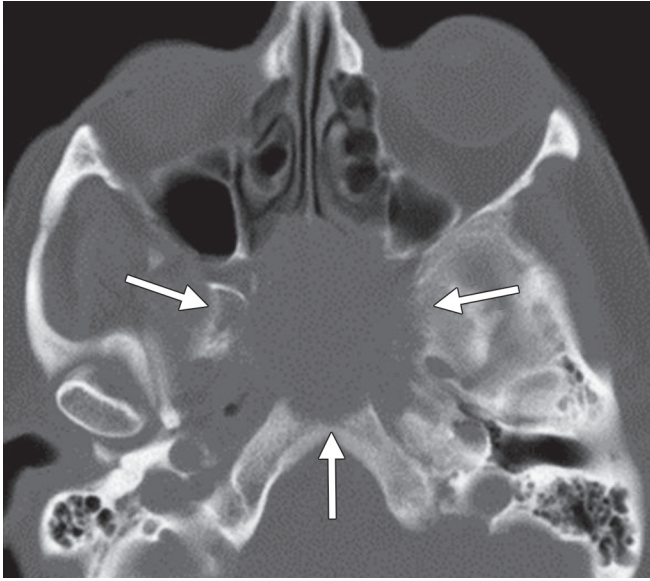
Fig. 3.16: Osseous erosion. Axial CT demonstrates a sphenoid sinus lesion eroding the clivus. Note the margin is irregular and infiltrative (arrows), highly suggestive of an aggressive tumor.

accompanying mass may reflect chronic granulomatous disease or prior surgery. While specific for aggression, absence of bone erosion should not dissuade further work-up; approximately 20% of squamous cell carcinomas (SCC), the most common malignant sinonasal tumors, do not demonstrate osseous destruction on presentation.[19]

CT Soft Tissues

Density

Much as the celsius temperature scale is defined by the freezing and boiling points of water at 0° and 100°, respectively, density on CT is measured in Hounsfield units (HU), a linear scale of electron density where 0 corresponds to water and the much lower density of air is defined as –1,000. Bone is typically 200–400 HU, whereas fat usually measures –100 to –20 HU, varying with contents, such as water from edema, and soft tissue elements.

Fat Density

The differential for a fat density lesion is relatively short and includes: herniated fat related to a bony defect, such as dehiscence of the lamina papyracea with medial protrusion of orbital fat into the ethmoid sinus, fat-packing from prior surgery, or a fat-containing mass, such as dermoid, teratoma, lipoma, or rarely liposarcoma.

Certain midline structures may normally but unexpectedly contain fat.
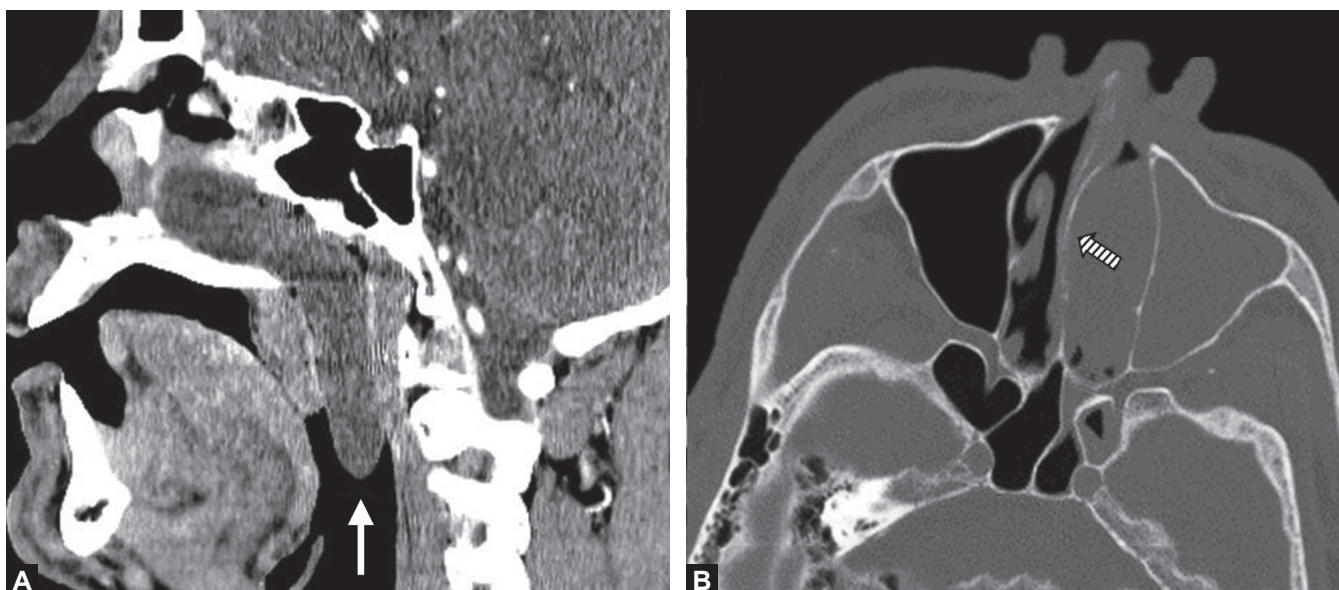
Fluid Density

Normal sinus secretions are predominantly water, with scant protein, and hence normally measure approximately water in density (typically 0 to 20 HU). With accretion and dehydration, sinus secretions may become heterogeneous and significantly denser, although inspissated mucus may be surrounded by relatively hypoattenuating new secretions.

The appearance of a rounded, homogeneous fluid density on CT (typically 0 to 20 HU) is most compatible with a mucus retention cyst or mucocele. Mucoceles, while benign, are typically associated with bulging and thinning (or demineralization) of adjacent bone, and may expand intracranially or intraorbitally, generating symptoms through mass effect (Fig. 3.15). Mucus retention cysts, which are much more common, usually do not remodel adjacent bone, but rarely may become displaced and cause obstruction.

A fluid density mass with smooth, lobulated, or polypoid contours may also represent a polyp (Figs. 3.17A and B). Specifically, extension of a polypoid fluid density mass through the maxillary ostium with nonerosive bony remodeling (possibly inclusive of the septum and turbinates) is strongly suggestive of an "antrochoanal polyp."

Diffuse opacification of the sinuses may reflect sinusitis or polyposis, which may or may not be distinguished by contours, pattern of enhancement or presence of osseous involvement.

Fluid density within the paranasal sinuses does not always represent mucoid secretions, and may instead reflect a CSF leak or meningocele. It is especially important to evaluate for underlying bone dehiscence at the anterior cranial fossa and pterygoid process of the sphenoid sinus, where CSF leaks are relatively common.[13] CT cisternography may be useful in identifying the site of a CSF leak if a diagnosis remains elusive. In this procedure, intrathecal contrast is administered through a lumbar puncture and is expected to pool at the site of a putative CSF leak, extending through the defect and into the sinus (Figs. 3.18A and B). Certain MRI protocols (specifically heavily-T2 weighted sequences such as 3D FIESTA) may also be helpful in better defining local anatomy, and assist in distinguishing a CSF leak from other lesions, such as a mucocele or simple sinus disease (Fig. 3.19).[20,21]

Figs. 3.17A and B: Polyp. (A) Sagittal CT (reconstruction) demonstrates a homogenous fluid density (HU 0-20), with smooth, ovoid contours drooping into the oropharynx (white arrow). (B) Bone kernel axial CT demonstrates benign-appearing bony remodeling (striped arrow) without evidence of erosion compatible with a polyp.

Soft Tissue Density

The appearance of soft tissue density (HU greater than what would be expected for water but less than 80) is most suggestive of cellular or proteinaceous contents, such as a tumor, although history of recent trauma, evidence of traumatic injury or layering density should suggest the possibility of blood products.

The most common sinonasal tumors in adults include: SCC, inverted papilloma (IP), adenocarcinoma, adenoid cystic carcinoma (ACS), sinonasal undifferentiated carcinoma (SNUC), esthesioneuroblastoma, melanoma, sarcoma, lymphoma, and metastases. In children, the most common sinonasal tumors include: juvenile nasopharyngeal angiofibroma (JNA), neurogenic tumors, papilloma, Langerhan's cell hystiocytosis, sarcoma, carcinoma, lymphoma, esthesioneuroblastoma, and metastases (especially neuroblastoma).

Tumors are typically soft tissue in density, although they may contain cystic (fluid-density) components, which may or may not be related to necrosis. It may be difficult to distinguish the borders of a soft tissue density mass from trapped mucus secretions on CT, a role better suited for MRI. Tumors may also contain calcifications, which may reflect the residua of eroded bony walls or nonspecific tumoral calcification.

The apparent center of a lesion, with consideration of mass effect and anatomic impedance to growth, may suggest underlying histology, as certain tumors have strong predispositions to origin or common patterns of disease extension.

Inverted papillomas for example are most commonly centered at the lateral wall of the nasal cavity, often near the middle turbinate and maxillary ostium (Figs. 3.20A to D).

Juvenile nasopharyngeal angiofibromas are hypervascular masses thought to arise from the sphenopalatine foramen. They typically expand the pterygopalatine fossa and subsequently may extend to the masticator space (Chandler's, Fisch's, and Radkowski's stage II). In advanced, stage III disease, intraorbital or intracranial extension may also be seen. Of note, involvement of the skull base is associated with early recurrence.[22,23]

A destructive, heterogeneous lesion centered at the cribriform plate is a common appearance of an esthesioneuroblastoma (olfactory neuroblastoma). These masses may extend to the orbit, which may underly exophthalmos, ophthalmoplegia, and visual loss. Inferior extension may also be seen, with erosion of the nasal septum. Cysts may be seen along the superior tumor margin, especially within the anterior cranial fossa.[24]

Hyperdensity

Very dense sinus contents (>80 HU) should strongly suggest the presence of fungus, with its elevated mineral content. This may reflect simple AFS, which may be accompanied by wall thickening or chronic deformation/expansion (Figs. 3.21A and B), or aggressive fungal

Figs. 3.18A and B: Four years following repair of a CSF leak patient returns with rhinorrhea and concern for recurrent CSF leak. Postoperative changes make the interpretation of this area difficult on (A) axial T2 MRI. (B) Axial CT cisternogram demonstrates hyperattenuating contrast (arrow) extending from the left middle cranial fossa into the lateral recess of the left sphenoid sinus, consistent with CSF leak.
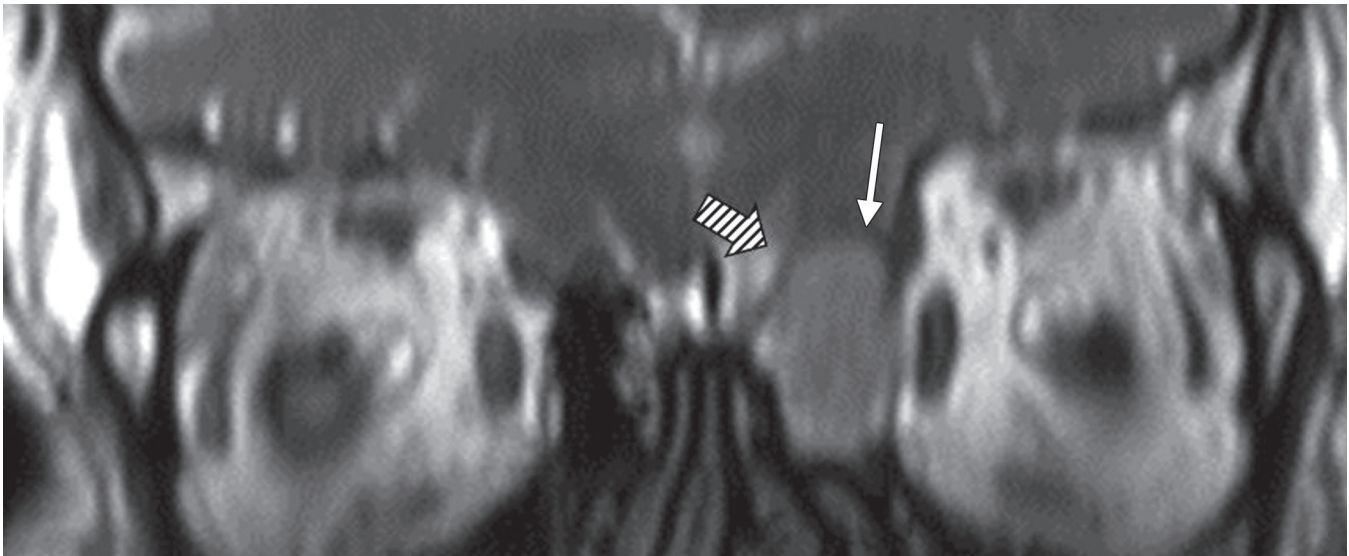

Fig. 3.19: High resolution coronal 3D FIESTA, a fluid-sensitive sequence, can be helpful to better visualize adjacent structures. In this patient with ethmoid mucocele (white arrow), the integrity of the olfactory groove (striped arrow) and the olfactory bulb can be demonstrated to better advantage.

disease, which is expected to demonstrate accompanying bony erosion. Desiccated mucus secretions may also be relatively hyperdense.

Enhancement

Enhancement on CT is related to a structure gaining density through perfusion by intravenously administered hyperdense contrast. Hence, the degree of enhancement is intimately related to contrast dose and vascularity, which equates with the propensity of a mass to bleed after biopsy. Any linear or branching avidly enhancing structure should be suspected of being vascular, and should not be biopsied or otherwise violated without due precaution.

Typically, tumors demonstrate internal "mass-like" and often heterogeneous enhancement, whereas mucosa
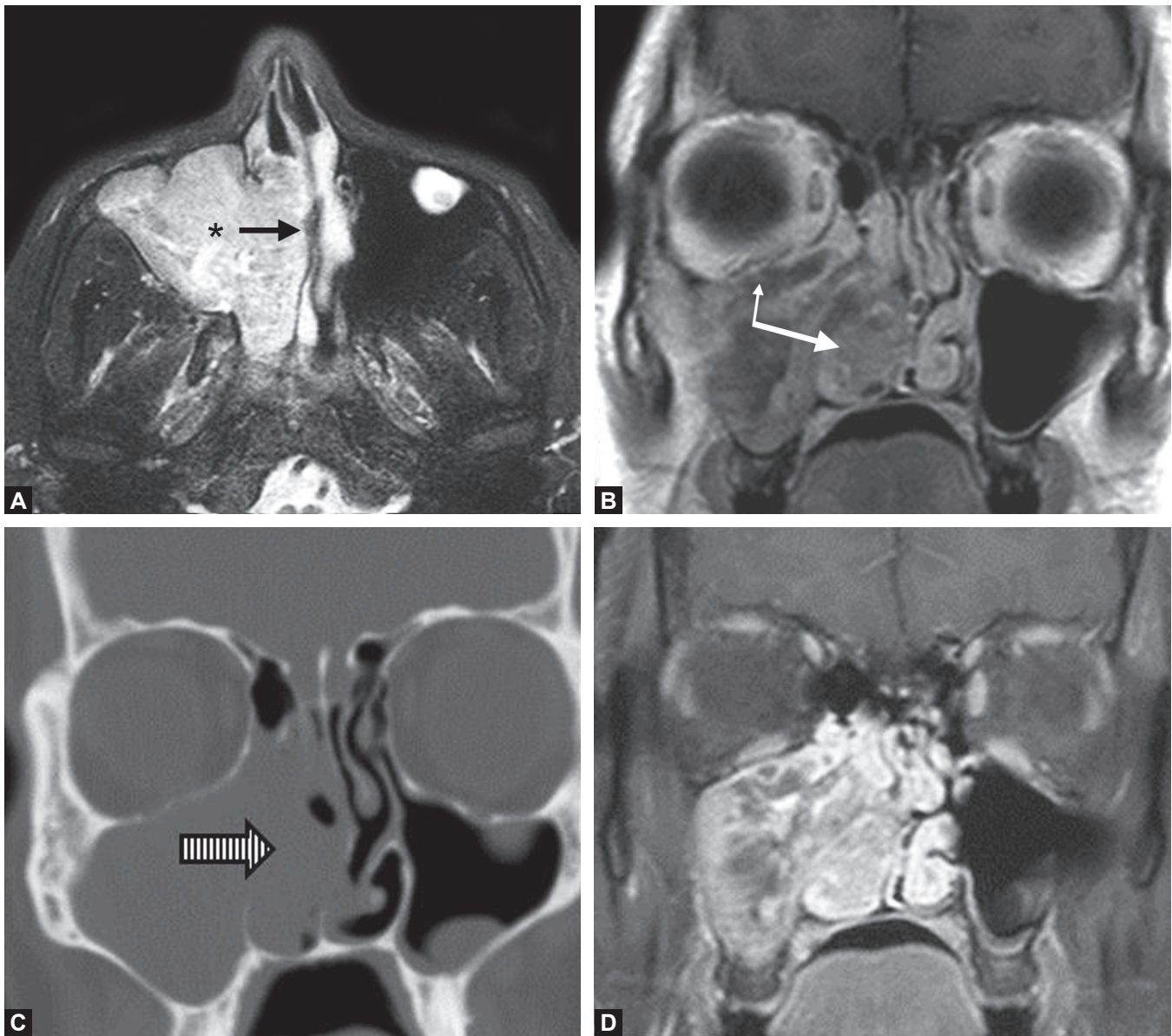
Figs. 3.20A to D: Inverted papilloma (IP) with focal transformation into squamous cell carcinoma (SCC). (A) Axial T2 demonstrates a hyperintense mass lesion expanding the right maxillary sinus (*), with bowing of the nasal septum (black arrow). (B) Coronal T1 precontrast shows remodeling of the orbital floor, with suggestion of destruction of the right inferior and middle turbinates and as well as the medial wall of the right maxillary sinus (double white arrows). Erosive changes are confirmed on (C) Coronal CT (striped arrow), suggesting an aggressive process concurrent with more indolent mass effect. (D) T1 postcontrast shows mass-like enhancement centered in the nasal cavity, as well as nonenhancing trapped sinus secretions in the maxillary sinus.

and abscesses demonstrate relatively homogeneous peripheral enhancement.

Hypervascular tumors, such as JNAs, demonstrate intense homogeneous enhancement, whereas nonhypervascular tumors may heterogeneously or minimally enhance. Differences in pattern of enhancement may be related to heterogeneity in feeding vessel vascularity, necrosis, or presence of cystic components, which do not enhance. Angiography is a useful adjunct modality that can more directly demonstrate the vascularity of a lesion, and may assist in preoperative planning, including embolization.

Magnetic Resonance Imaging

Magnetic resonance imaging relies on the differences in magnetic properties of hydrogen in various molecular
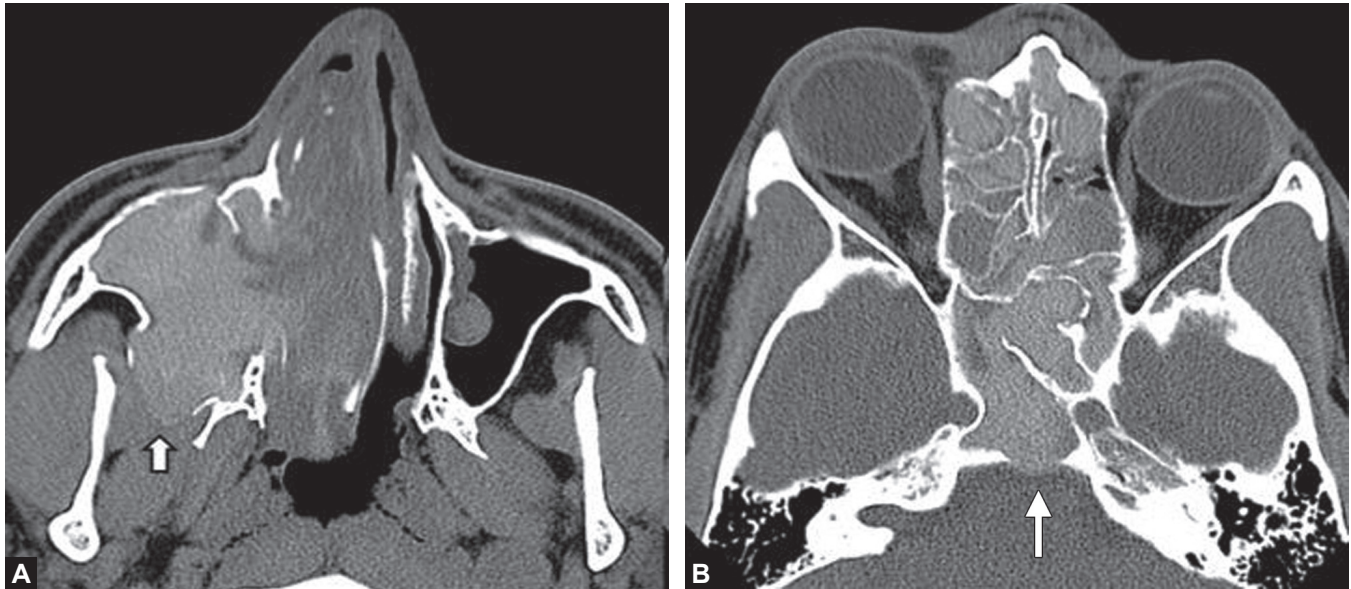
Figs. 3.21A and B: Axial CT images demonstrate diffuse sinus disease with focal expansion and pressure demineralization of the posterior walls of the (A) right maxillary and (B) right sphenoid sinuses (arrows) compatible with chronic, and specifically allergic fungal sinusitis (AFS). Hyperdensity of sinus contents, appreciated on these soft-tissue windows, further supports the presence of fungus.

environments to generate contrast between tissues. While lacking the spatial resolution of CT, and suffering from local field distortion related to paramagnetic effects (iron, air, calcium), MRI has excellent soft tissue contrast as well as the ability to typify molecular environment (e.g., DWI and spectroscopy).

Magnetic resonance imaging particularly excels in characterizing soft tissue masses, such as in discriminating between postobstructive secretions, tumor tissue and scarring, and is able to precisely define tumor extent, including early bone marrow involvement and perineural spread.[25,26] MRI may demonstrate intraosseous extension of a tumor or aggressive infection even before osseous changes in the form of cortical erosion are apparent on CT, especially at the skull base.[25]

It should be emphasized that MRI is not a screening tool, but rather a problem-solving tool. This is because osseous cortical erosion, a hallmark of aggressive sino-nasal pathology, is often exceedingly subtle or invisible on MRI, while usually adequately visualized on CT. Nevertheless, lesion appearance and extent on both CT and contrast-enhanced MRI is useful in refining a differ-ential diagnosis if a lesion is identified, and may critically impact the therapeutic approach.

Different MRI sequences or protocols rely on various molecular properties of tissues, and have distinct stren-gths and weaknesses. In concert, they are very useful in solving a variety of diagnostic problems.

T2

This primary diagnostic sequence is especially sensitive to fluid content. Fluid-containing structures are hyper-intense (bright) on T2-weighted sequences, hence inflam-matory lesions are often homogeneous and T2-hyper-intense.[27] As fluid is replaced by protenaceous content or hemorrhage, whether inspissated mucus or tumor, T2 signal decreases.

Although the majority (80%) of malignant sinonasal cavity tumors are SCC, which have intermediate T2 signal, 10% are hypercellular tumors (lymphomas, olfactory neuroblastomas/PNET, etc.), which have little water con-tent, and appear low to intermediate signal intensity on T2-weighted imaging. Conversely, salivary gland tumors usually have intermediate to high T2-signal, whereas schwannomas are often T2-hyperintense, occasionally with a "*target sign*" appearance typical of an epineurial capsule: low central T2 signal surrounded by high T2 signal intensity. In contrast, neurofibromas are usually not encapsulated, and hence do not demonstrate peripheral T2 hyperintensity.[28] These examples illustrate that both signal intensity and overall appearance may be helpful in refining a differential diagnosis. They furthermore stress that T2-hyperintensity is not equivalent to fluid collection, as some tumors may be T2-hyperintense, but are distinguished by contrast enhancement.[29]

Tissues lacking water, including bone, air and cartilage, appear dark on T2-weighted sequences, as do structures
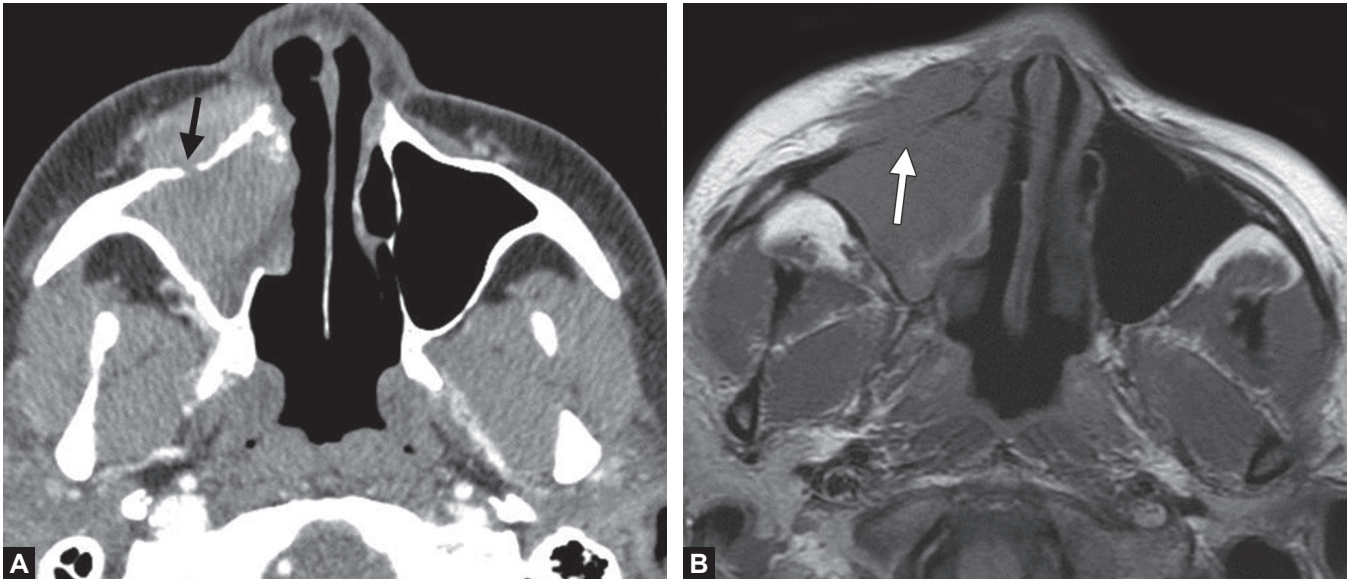
Figs. 3.22A and B: (A) Axial postcontrast CT demonstrates a soft tissue mass in the right maxillary sinus, eroding through the anterior wall (black arrow), which highlights the aggressive nature of this lesion. Although noncontrast axial T1-weighted imaging (B) also demonstrates the osseous erosion (white arrow), the replacement of the expected T1 hyperintense preantral fat by tumor is more apparent.

where signal is lacking for reasons related to high-velocity flow ("flow voids") or magnetic distortion. Magnetic distortion or signal loss may be caused by macroscopic metal (from hardware, foreign bodies), or microscopic minerals within cells, whether related to iron-avid fungus or macrophages associated with hemorrhage or abscess.

T1

This sequence primarily benefits from the native T1-hyperintensity of fat-containing tissues, including the regions surrounding the maxillary sinuses, the orbital contents, and bone-marrow. Replacement of the normally T1-bright premaxillary fat may be the first sign of an aggressive process within the maxillary sinus (Figs. 3.22A and B). Similarly, loss of expected T1-hyperintensity in the orbital apex can be an early indication of aggressive fungal sinusitis. Abnormal marrow signal can be more difficult to interpret, as aggressive and reactive changes may appear similar, and subtle bony erosion may be difficult to appreciate on MRI. In such cases, correlation with CT can be of great value.

In addition to fat, highly protenaceous collections, recent blood products, and various biological cations associated with necrosis (including copper, iron, and manganese) may appear bright on T1-weighted sequences, as can melanin and slow vascular flow. These can usually be distinguished by findings from other MRI sequences, as well as by additional information obtained from CT.

It should be noted that the MRI appearance of calcification varies by the specific molecular form of calcium, which is often not visible for technical reasons. If calcification is seen it usually appears (1) T2-hypointense due to associated paramagnetic ions, (2) dark on all sequences due to lack of mobile water, or (3) hyperintense on T1-weighted imaging.

Contrast-Enhanced MRI

Contrast-enhanced sequences usually refer to T1-weighted sequences obtained following IV administration of gadolinium-containing contrast and employing fat-saturation techniques. Hence, it is important to compare postcontrast sequences to fat-saturated precontrast T1-weighted sequences to evaluate enhancement and to avoid diagnostic blunders.

Contrast-enhanced T1-sequences are superb in delineating lesion extent and margins, which may critically impact therapeutic approach. Postcontrast sequences are helpful in differentiating a T2-hyperintense mass from a cyst, and are likewise useful in distinguishing mass from adjacent retained secretions and scar tissue. Diagnostically it is especially important to distinguish the smooth contours of mucosal enhancement, and thick rim enhancement of abscesses, from mass-like enhancement
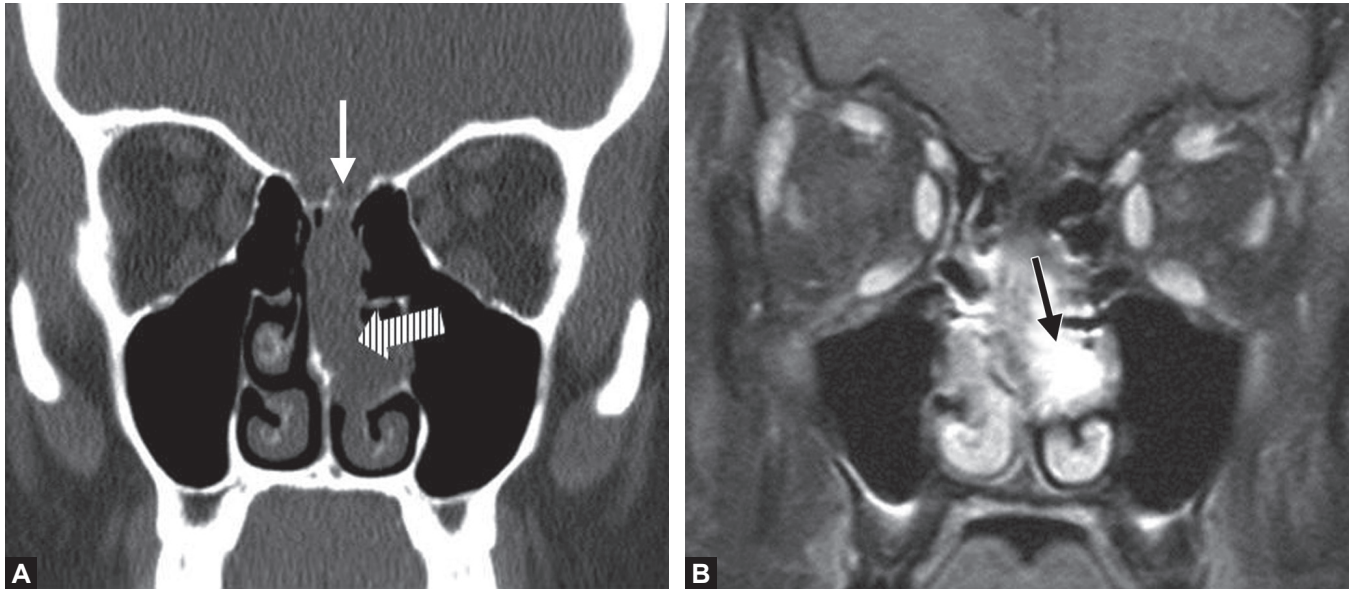
Figs. 3.23A and B: (A) Coronal CT demonstrates nonspecific opacity below the left cribriform plate (white arrow), which can be easily mistaken for sinus secretions. Note the absence of left middle turbinate (striped arrow) which is worrisome for erosion from an aggressive process. Postcontrast coronal T1 (B) demonstrates an enhancing mass (black arrow). The differential for mass enhancement in this region includes squamous cell carcinoma (SCC), hemangipericytoma, esthesioneuroblastoma, sinonasal undifferentiated carcinoma (SNUC), and lymphoma.

of tumors (Figs. 3.23A and B). Contrast-enhanced MR imaging may also help to grade mass vascularity, which may be useful for preoperative planning.

Postcontrast images can also improve detection of perineural spread of a tumor. In patients with tumors such SCC and sinonasal ACC, which have a high predilection for perineural spread, close attention should be paid to trigeminal nerve branches within the pterygopalatine fossa, as enhancement within foramen rotundum, infraorbital fissure (V2), and foramen ovale (V3) are strongly suggestive of perineural spread.

Diffusion-Sensitive Sequences

Diffusion-weighted imaging is a T2-weighted sequence that is sensitive to the microscopic flow of water molecules. In regions where this flow is limited or "restricted" the DWI signal will be bright. The same region will appear dark on a mathematically calculated complementary sequence called apparent diffusion coefficient (ADC).

Restricted diffusion typically reflects hypercellularity (decreased extracellular water, and high nuclear to cytoplasmic ratio in a mass) or (highly protenaceous) viscous fluid.

A diffusion-restricting, enhancing mass centered within the sinonasal cavity most likely represents lymphoma, a prototypical hypercellular mass, which often

has a bulky appearance, demonstrates hypointense signal on T2-weighted imaging, and moderate enhancement (Figs. 3.24A to C). Lymphomas, especially high grade lymphomas, may remodel or destroy bone (e.g., nasal septal perforation is often associated with nasal T-cell lymphomas), hence it is important to look for signs of osseous involvement on CT bone windows and MRI T1 sequences. Other typically hypercellular tumors include neuroblastoma, fibrous histiocytoma, and sarcoma.

Viscous fluid collections, such as highly proteinaceous mucous retention cysts and abscesses, will also restrict diffusion. Postcontrast sequences can help distinguish these from hypercellular masses, which should demonstrate solid, "mass-like" enhancement, as opposed to rim enhancement of fluid collections (Figs. 3.25A to D).[30]

The appearance of DWI signal hyperintensity without corresponding low signal on ADC sequences likely reflects "T2 shine-through," an artifact related to underlying T2 signal hyperintensity rather than restricted diffusion.

Complementary Modalities

Positron emission tomography (PET) is a physiologic test, which measures relative glucose metabolism in tissues, and relies on the notion that standard uptake values are elevated in tumors and inflammatory processes
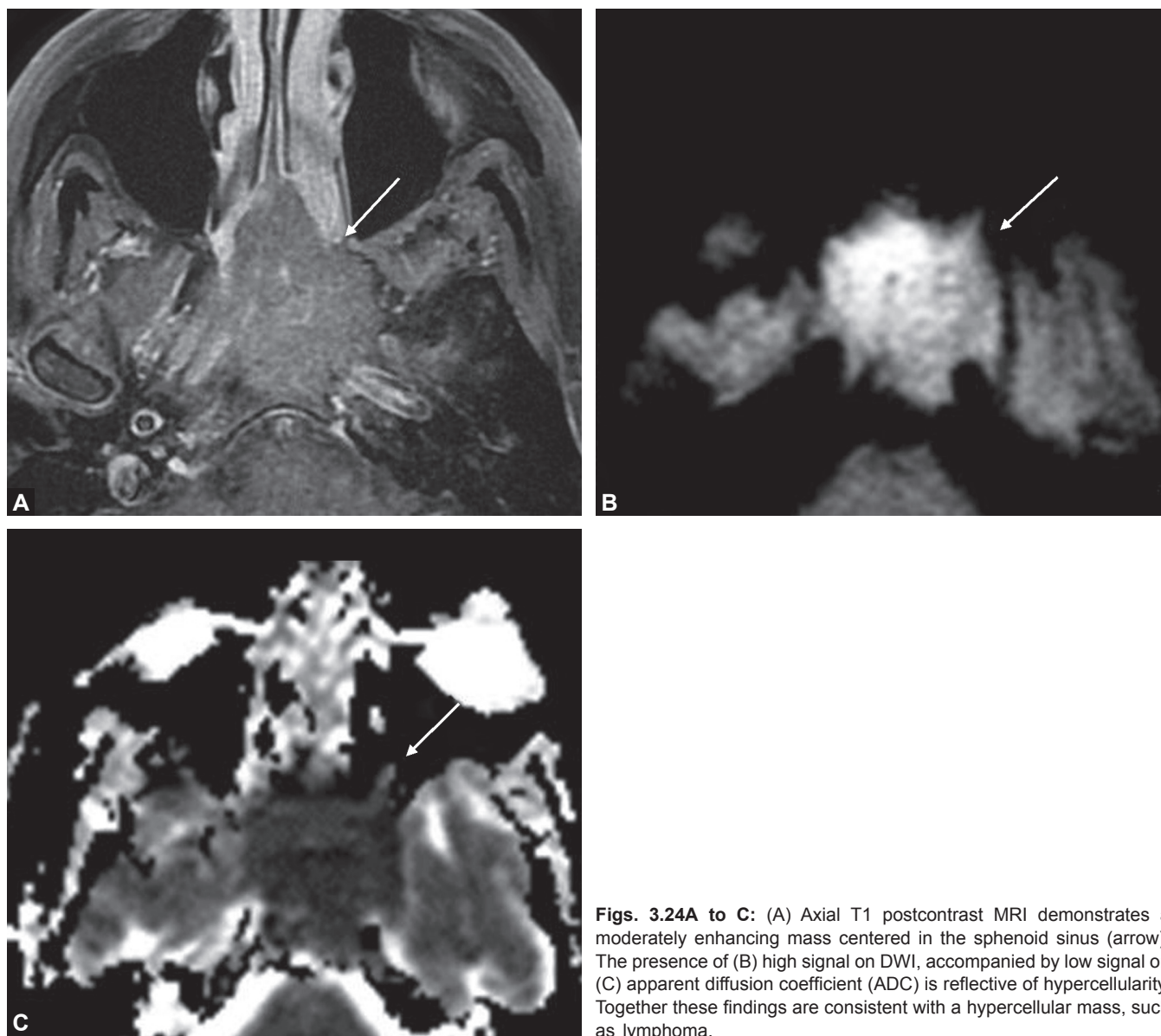
Figs. 3.24A to C: (A) Axial T1 postcontrast MRI demonstrates a moderately enhancing mass centered in the sphenoid sinus (arrow). The presence of (B) high signal on DWI, accompanied by low signal on (C) apparent diffusion coefficient (ADC) is reflective of hypercellularity. Together these findings are consistent with a hypercellular mass, such as lymphoma.

(Fig. 3.26). PET may be useful for discriminating between postirradiative changes and tumor recurrence; however, its low spatial resolution limits its sensitivity for local disease and small masses. Although PET may confirm presence of a tumor in the sinonasal cavity, its primary role is the detection of distal metastases or systemic involvement in granulomatous disease.[31]

Angiography is an adjunct modality that may lead to a more accurate diagnosis if a vascular mass is suspected, and which may facilitate preoperative embolization to reduce risk of hemorrhage (Figs. 3.27A to C).

CONCLUSIONS

The essence of an effective radiologic approach to the sinonasal region rests on a thorough knowledge of the anatomy and a basic understanding of the relevant imaging modalities combined with a reasoned, systematic reading pattern. While knowledge of typical features of common entities may be helpful in narrowing the differential diagnosis, the goal of imaging should be to solve essential problems of screening: distinguishing normal from abnormal, chronic versus acute, focal from diffuse, and indolent from aggressive.
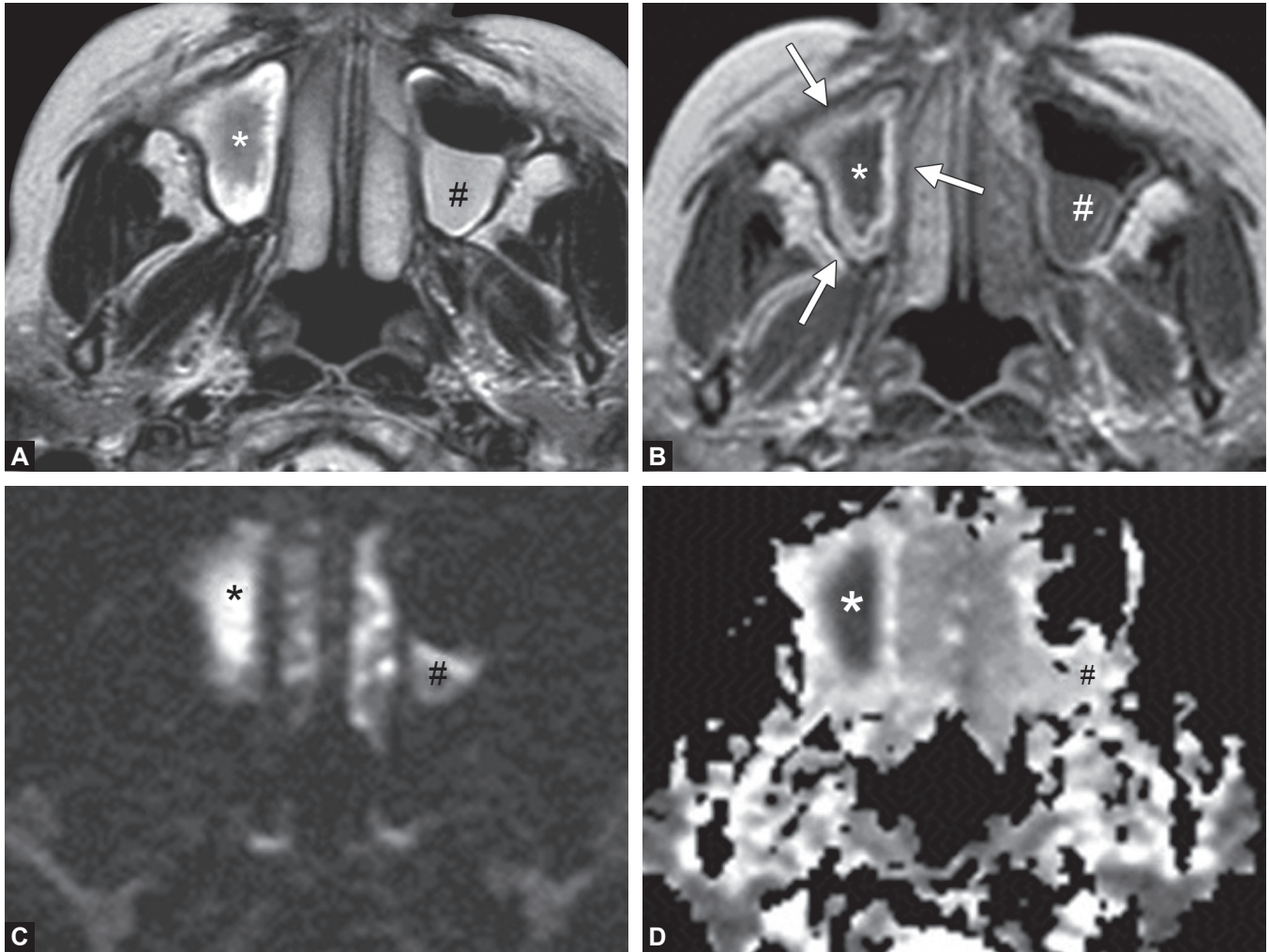
Figs. 3.25A to D: (A) Axial T2-weighted, (B) T1 postcontrast, (C) DWI, and (D) ADC images demonstrate that restricted diffusion does not always relate to hypercellularity. In this case, flow is restricted due to a viscous effusion reflecting acute on chronic sinusitis. This is supported by the rim enhancement (arrows) of the sinus mucosa and absence of enhancement of the area that demonstrates restricted diffusion (*). An abscess would also demonstrate restricted diffusion and rim enhancement but would be centrally T2 hyperintense reflecting its fluid content, rather than T2 hypointense reflecting inspissated fluid. Note the relatively simple fluid in the left maxillary sinus (#).
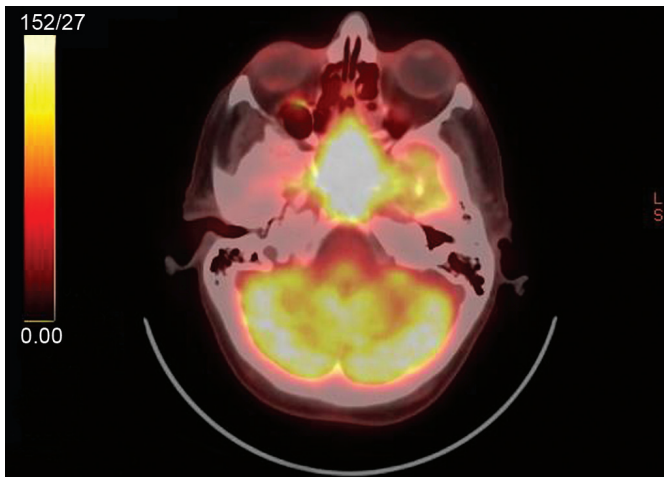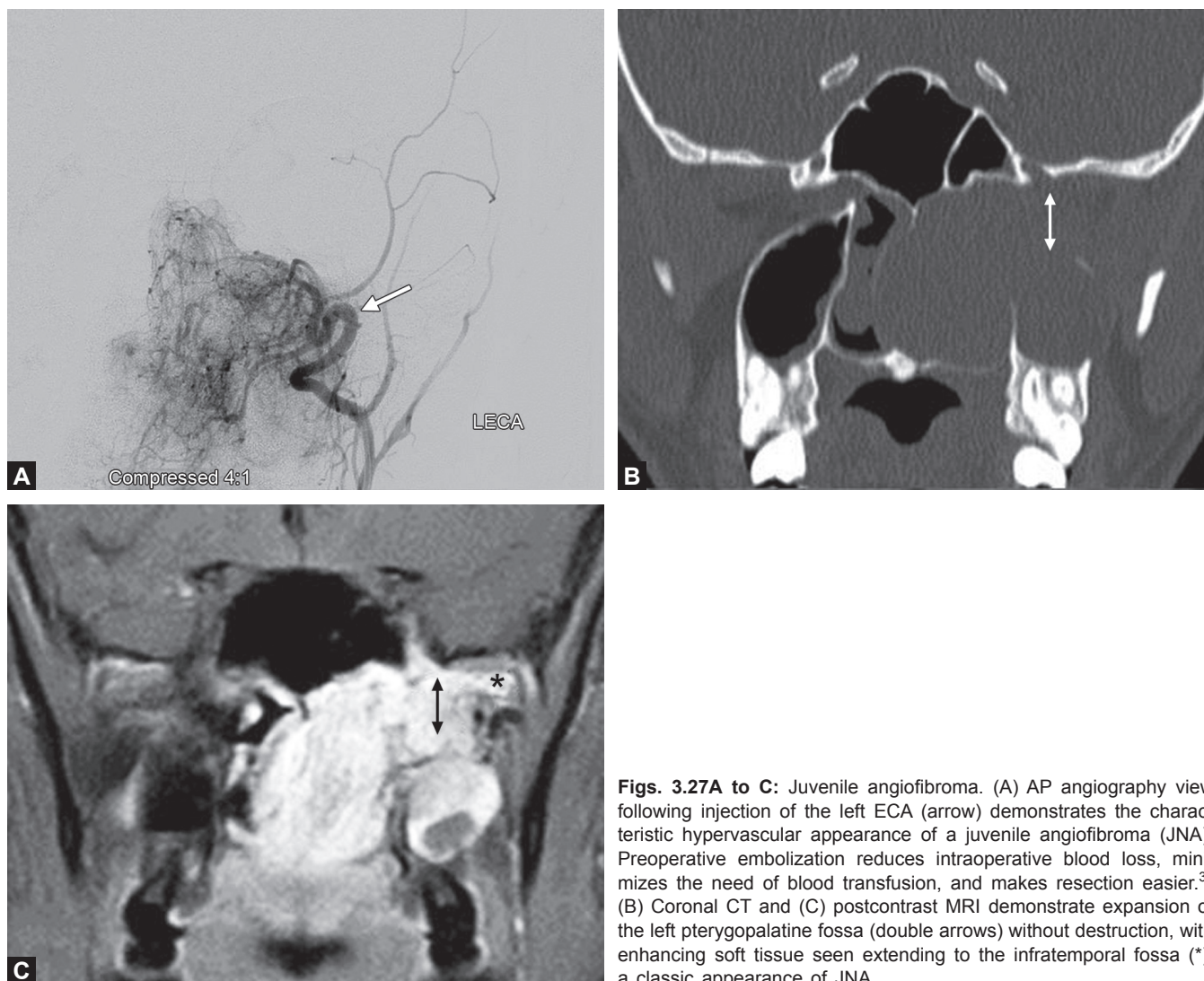

Fig. 3.26: Fusion of axial CT and PET demonstrates marked FDG uptake in the sphenoid sinus representing a hypermetabolic mass, in this case a biopsy-proven lymphoma.

Figs. 3.27A to C: Juvenile angiofibroma. (A) AP angiography view following injection of the left ECA (arrow) demonstrates the characteristic hypervascular appearance of a juvenile angiofibroma (JNA). Preoperative embolization reduces intraoperative blood loss, minimizes the need of blood transfusion, and makes resection easier.[32] (B) Coronal CT and (C) postcontrast MRI demonstrate expansion of the left pterygopalatine fossa (double arrows) without destruction, with enhancing soft tissue seen extending to the infratemporal fossa (*), a classic appearance of JNA.

REFERENCES

1. Som PS, Curtin HD (Eds). Head and Neck Imaging, Vol. 1. St. Louis: CV Mosby; 2003. pp. 87-147.
2. Ruíz DSM, Gailloud P, Rüfenachta DA, et al. Anomalous intracranial drainage of the nasal mucosa: a vein of the foramen caecum? AJNR Am J Neuroradial. 2006;27:129-31.
3. Singh A, Wessell AP, Anand VK, et al. Surgical anatomy and physiology for the skull base surgeon. Operative Techn Otolaryngol. 2011;22:184-93.
4. Beale TJ, Madani G, Morley SJ. Imaging of the paranasal sinuses and nasal cavity: normal anatomy and clinically relevant anatomical variants. Semin Ultrasound CT MR. 2009;30(1):2-16.
5. Reddy UD, Dev B. Pictorial essay: Anatomical variations of paranasal sinuses on multidetector computed tomography-How does it help FESS surgeons? Indian J Radiol Imaging. 2012;22(4):317-24.
6. Santiago R, Villalonga P, Maggioni A. Nasal septal abscess: A case report. Int Pediatr. 1999;14:229-31
7. Maroldi R, Nicolai P (Eds). Imaging in Treatment Planning for Sinonasal Diseases. Berlin: Springer-Verlag; 2005.
8. Reeder MR, Bradley, WG Jr., Merritt CR. Reeder and Felson's Gamuts in Radiology and 4.0 Web Version: Comprehensive Lists of Imaging Differential Diagnoses; 2003.
9. Keros P. On the practical value of differences in the level of the lamina cribrosa of the ethmoid. Z Laryngol Rhinol Otol. 1962;41:809-13.
10. Sonkens JW, Harnsberger HR, Blanch GM, et al. The impact of screening sinus CT on the planning of functional endoscopic sinus surgery. Otolaryngol Head Neck Surg. 1991; 105:802-13.
11. Sirikci A, Bayazit YA, Bayram M, et al. Variations of sphenoid and related structures. Eur Radiol. 2000;10(5):844-8.
12. Fernandez-Miranda JC, Prevedello DM, Madhok R, et al. Sphenoid septations and their relationship with internal

carotid arteries: anatomical and radiological study. Laryngoscope. 2009;119(10):1893-6.

13. Shetty PG, Shroff MM, Fatterpekar GM, et al. A retrospective analysis of spontaneous sphenoid sinus fistula: MR and CT findings. AJNR Am J Neuroradiol. 2000;21:337-42.

14. Sindou M (Ed). Practical Handbook of Neurosurgery: From Leading Neurosurgeons, Vol. 1. New York: Springer-Verlag; 2009. p. 203.

15. Rao VM, El-Noueam KI. Sinonasal imaging. Radiol Clin North Am. 1998;36(5):921-39.

16. Illner A, Davidson HC, Harnsberger HR, et al. The silent sinus syndrome: clinical and radiographic findings. AJR 2002;178:503-6.

17. Reddy GSP, Kumar BS, Muppa R, et al. Odontogenic fibromyxoma of maxilla: a rare case report. Case Rep Dent. 2013; 2013:345479.

18. Jackson AR. Bone thinning in frontal mucocele. Br J Radiol. 1977;50(591):181-4.

19. Kennedy DW, Bolger WE, Zinreich SJ (Eds). Diseases of the Sinuses: Diagnosis and Management. Ontario: BC Decker; 2001. p. 145.

20. Stone JA, Castillo M, Neelon B, et al. Evaluation of CSF leaks: high-resolution CT compared with contrast-enhanced CT and radionuclide cisternography. AJNR 1999;20:706-12.

21. Tyagi I, Syal R, Goyal A. Cerebrospinal fluid otorhinorrhoea due to inner-ear malformations: clinical presentation and new perspectives in management. J Laryngol Otol. 2005;119(9):714-8.

22. Radkowski D, McGill T, Healy GB, et al. Angiofibroma. Changes in staging and treatment. Arch. Otolaryngol. Head Neck Surg. 1996;122 (2):122-9.

23. Kania RE, Sauvaget E, Guichard JP, et al. Early Postoperative CT scanning for juvenile nasopharyngeal angiofibroma: detection of residual disease. AJNR 2005;26:82-8.

24. Broich G, Pagliari A, Ottaviani F. Esthesioneuroblastoma: a general review of the cases published since the discovery of the tumour in 1924. Anticancer Res. 1997;17(4A):2683-706.

25. Nemzek WR, Hecht S, Gandour-Edwards R, et al. Perineural spread of head and neck tumors: how accurate is MR imaging? AJNR Am J Neuroradiol. 1998;19:7016.

26. Shy CG, Chen CC, Chen WH, et al. Comparison of CT with MRI for the evaluation of the juxta-oral tumor. Chin J Radiol. 2003;28:1-8.

27. Hurt CJ, Yousem DM, Beauchamp NJ (Eds). Head and Neck. Holland-Frei Cancer Medicine, 6th edition. Hamilton, Ontario: BC Decker; 2003.

28. Koga H, Matsumoto S, Manabe J, et al. Definition of the target sign and its use for the diagnosis of schwannomas. Clin Orthop Relat Res. 2007;464:224-9.

29. Genden EM, Varvares MA (Eds). Head and Neck Cancer: An Evidence-Based Team Approach. Thieme, 2008. Carcinoma of the Nasal Cavity and Paranasal Sinus.

30. Chawla S, Kim S, Wang S, et al. Diffusion-weighted imaging in head and neck cancers. Future Oncol. 2009;5(7): 959-9.

31. Ramakrishnan VR, Lee JY, O'Malley BW Jr. et al. 18-FDG-PET in the initial staging of sinonasal malignancy. Laryngoscope. 2013;123(12):2962-6.

32. Giavroglou C, Constantinidis J, Triaridis S, et al. Angiographic evaluation and embolization of juvenile nasopharyngeal angiofibroma. HNO. 2007;55(1):36-41.